



# New evidence of an Ediacaran age for the Bambuí Group in southern São Francisco craton (eastern Brazil) from zircon U–Pb data and isotope chemostratigraphy



Gustavo Macedo Paula-Santos <sup>a,\*</sup>, Marly Babinski <sup>a</sup>, Matheus Kuchenbecker <sup>b</sup>, Sergio Caetano-Filho <sup>c</sup>, Ricardo Ivan Trindade <sup>d</sup>, Antonio Carlos Pedrosa-Soares <sup>b</sup>

<sup>a</sup> Instituto de Geociências, Universidade de São Paulo, Rua do Lago, 562, Cidade Universitária, São Paulo, SP CEP: 05508-080, Brazil

<sup>b</sup> Instituto de Geociências-CPMT, Universidade Federal de Minas Gerais, Av. Antônio Carlos, 6627, Campus Pampulha, Belo Horizonte, MG CEP: 31270-901, Brazil

<sup>c</sup> Instituto de Geociências e Ciências Exatas, Universidade Estadual Paulista, Av. 24A, Rio Claro, SP CEP: 13506-900, Brazil

<sup>d</sup> Instituto de Astronomia e Geofísica, Universidade de São Paulo, Rua do Matão, 1226, São Paulo, SP CEP: 05508-090, Brazil

## ARTICLE INFO

### Article history:

Received 13 December 2013

Received in revised form 16 June 2014

Accepted 28 July 2014

Available online 23 August 2014

Handling Editor: A.S. Collins

### Keywords:

Bambuí Group

São Francisco craton

U–Pb dating

Sr isotopes

## ABSTRACT

Extensive carbonate–siliciclastic successions of the Bambuí Group, which overlie Neoproterozoic glaciogenic diamictites, cover most of the southern São Francisco craton (eastern Brazil). This group records sedimentation in a foreland setting related to the diachronic orogenic processes that formed the Brasília and Araçuaí marginal belts. The lowermost unit of the Bambuí Group, the Sete Lagoas Formation, comprises two shallowing-upward sequences of carbonate rocks with subordinated pelitic intercalations, overlying the glaciogenic diamictites in the southern São Francisco Craton. This study combines isotope chemostratigraphy (C, O, Sr) and U–Pb dating of zircon detrital grains retrieved from marls of the Sete Lagoas Formation. The basal sequence comprises low organic matter limestones and dolostones with  $\delta^{13}\text{C}$  values around 0‰, positioned above cap carbonates dated at around 740 Ma (Pb–Pb whole-rock isochron). The U–Pb ages obtained for this sequence show several age peaks between 1270–870 Ma and 625–550 Ma. The upper sequence includes dark limestones with  $\delta^{13}\text{C}$  values as high as +10‰, best preserved  $^{87}\text{Sr}/^{86}\text{Sr}$  ratios of around 0.7075 and U–Pb ages ranging from 625 Ma to 550 Ma. Our geochronological data suggest that the Araçuaí orogen is the main source of sediment for the Sete Lagoas Formation, and the youngest zircon population sets the maximum depositional age for its upper part at around 557 Ma. This suggests that the studied section of the Sete Lagoas Formation is not related to either the Sturtian or the Marinoan glacial events. Also, the  $^{87}\text{Sr}/^{86}\text{Sr}$  ratios obtained from Sete Lagoas carbonates contrast with Sr evolution curves available in the literature, especially with those for the Ediacaran–Cambrian limit, when ratios higher than 0.7080 would be expected. The same discrepancy is reported for other Ediacaran carbonate successions, pointing to local disturbances in Sr composition of marine basins rather than global processes. Interbasinal correlations and blind dating based on isotope chemostratigraphy should proceed carefully, especially for Ediacaran marine deposits located on the inner parts of large palaeocontinental regions, such as those found in western Gondwana.

© 2014 International Association for Gondwana Research. Published by Elsevier B.V. All rights reserved.

## 1. Introduction

The São Francisco craton, together with its counterpart located in Africa, the Congo craton (Fig. 1), represents the stable part of one of the plates involved in the assembly process of western Gondwana, in the Neoproterozoic (Cordani et al., 2003). This long-lasting orogenic process, represented by the Brasiliano–Pan African event, formed diachronic mobile belts adjacent to those cratons, like the Araçuaí and Brasília belts that, respectively, place the east and west limits of the São Francisco craton (Brito-Neves et al., 1999). Around the Ediacaran–Cambrian boundary, the São Francisco craton and related orogenic

belts occupied a central place in the newborn western Gondwana (Trindade et al., 2006; Li et al., 2008). By that time, both the Araçuaí and Brasília belts have already been uplifted against the São Francisco craton, showing Neoproterozoic stratigraphic unit thrust onto the cratonic covers included in the Bambuí Group (Dardenne, 2000; Alkmim et al., 2006; Valeriano et al., 2008; Pedrosa-Soares et al., 2011a).

The Bambuí Group includes a thick (up to 1000 m) carbonate–siliciclastic succession covering a large region of the southern São Francisco Craton, in eastern Brazil (Fig. 1). The lithostratigraphic subdivision of the Bambuí Group into five formations (namely the Sete Lagoas, Serra de Santa Helena, Lagoa do Jacaré, Serra da Saudade and Três Marias Formations) suggested by Dardenne (1978) is still the most accepted in the literature (e.g., Santos et al., 2000, 2004; Alvarenga et al., 2007; Babinski et al., 2007; Vieira et al., 2007; Sial et al., 2009; Babinski et al., 2012).

\* Corresponding author.

E-mail address: [gustavomp@yahoo.com.br](mailto:gustavomp@yahoo.com.br) (G.M. Paula-Santos).

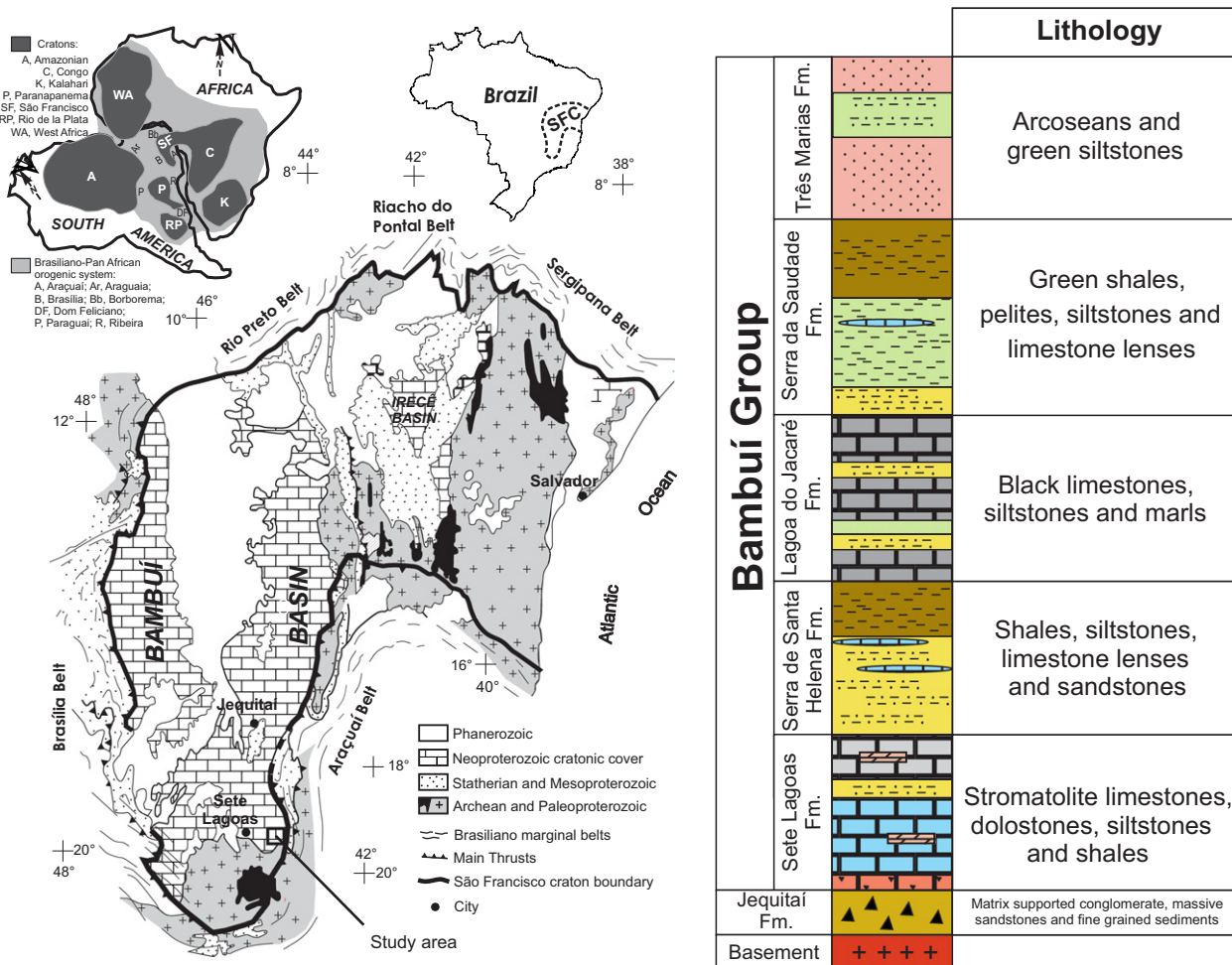


**Fig. 1.** Geological map of São Francisco craton with the paleogeographic reconstruction of West Gondwana (modified from Alkmim et al., 2006) and stratigraphic column of the Bambuí Group based on Dardenne (1978).

The Sete Lagoas Formation, the lowermost unit of the Bambuí Group, crops out close to basement highs in the southern part of the São Francisco craton (Fig. 1). This unit comprises two shallowing-upward sequences of carbonates with interbedded pelitic rocks (Vieira et al., 2007). The lower carbonates overlie glaciogenic diamictites and associated deposits correlated to the Jequitáí and Carrancas formations (Uhlein et al., 1999; Martins-Neto et al., 2001; Martins-Neto and Hercos, 2002; Vieira et al., 2007; Kuchenbecker et al., 2013). This stratigraphic framework established the Sete Lagoas Formation as one of the ‘cap carbonate’ successions deposited above glacial deposits that record Neoproterozoic extreme glacial events (Babinski et al., 2007; Vieira et al., 2007; Caxito et al., 2012). This is supported by the  $\delta^{13}\text{C}$  negative anomalies found within the base of the unit. Nevertheless, the sedimentary evolution, the age of the Sete Lagoas Formation and the glacial event which pre-dates the carbonate deposition have been themes of intense debate, mainly because of controversial arguments facing blind dating and absolute geochronological data.

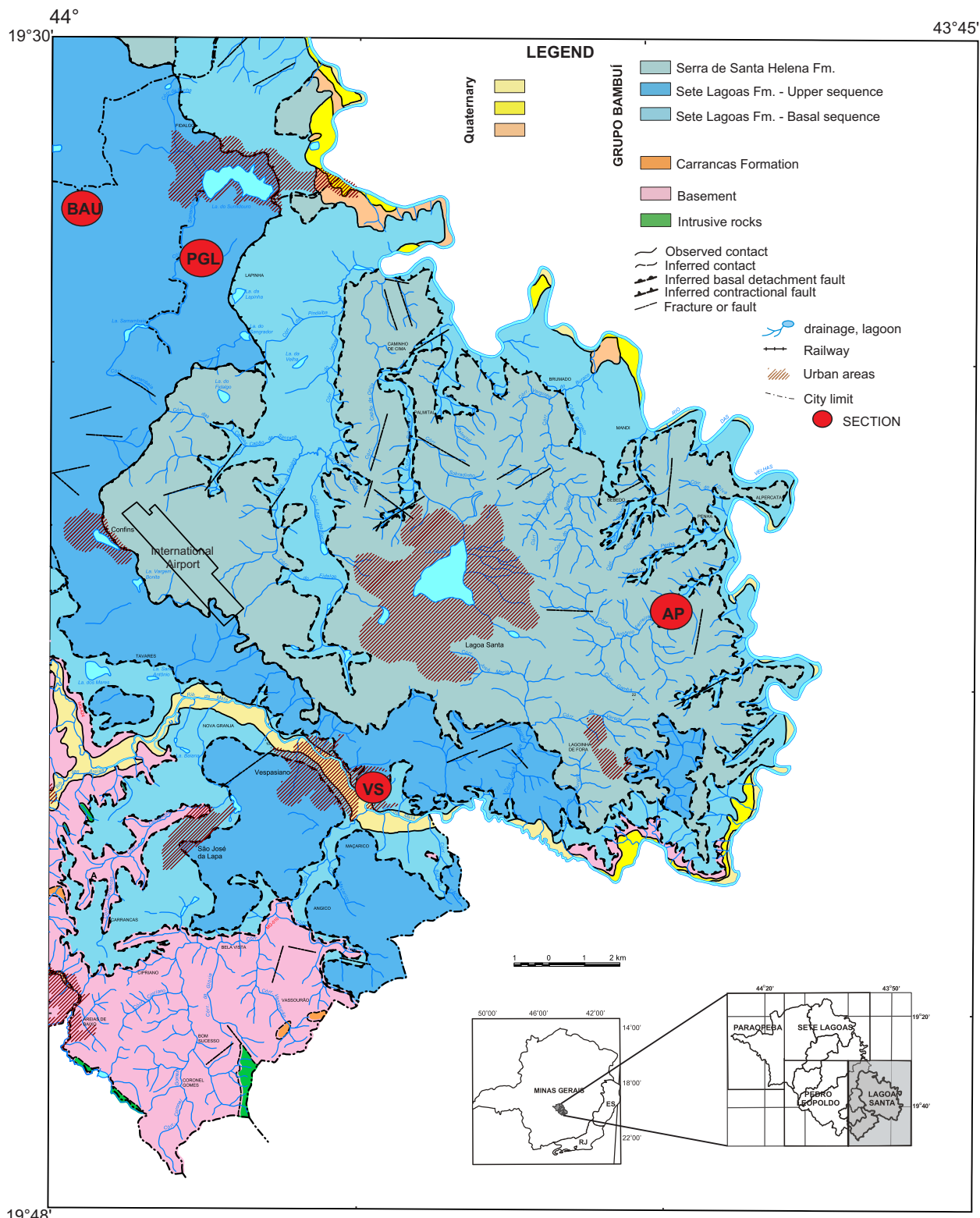
Babinski et al. (2007) obtained a  $^{207}\text{Pb}$ – $^{206}\text{Pb}$  isochron age of  $740 \pm 22$  Ma on the least altered samples of the basal cap carbonates and, therefore, considered the Sete Lagoas Formation as a post-Sturtian succession. Rodrigues (2008) and Pimentel et al. (2011) reported a maximum depositional age of 610 Ma after dating, by the U-Pb method, detrital zircons retrieved from pelitic layers of the upper sequence of the Sete Lagoas Formation, and correlate it with post-Marinoan carbonate successions. Recently, the Ediacaran guide fossil *Cloudina* has been described in these carbonates (Warren et al., 2014), bringing more pieces to the Bambuí Group puzzle. A possible major unconformity

between the lower and upper sequences of the Sete Lagoas Formation has been postulated, as such sequence boundary is characterized by an abrupt shift on the  $\delta^{13}\text{C}$  curve, from values around 0‰ to values higher than +6‰ (Santos et al., 2000; Vieira et al., 2007). However, no field evidence has been found. The geochronological data from older glacial units in the region do not help solve the puzzle, as their maximum depositional ages are around 900 Ma (Buchwaldt et al., 1999; Pedrosa-Soares et al., 2000; Babinski et al., 2012).

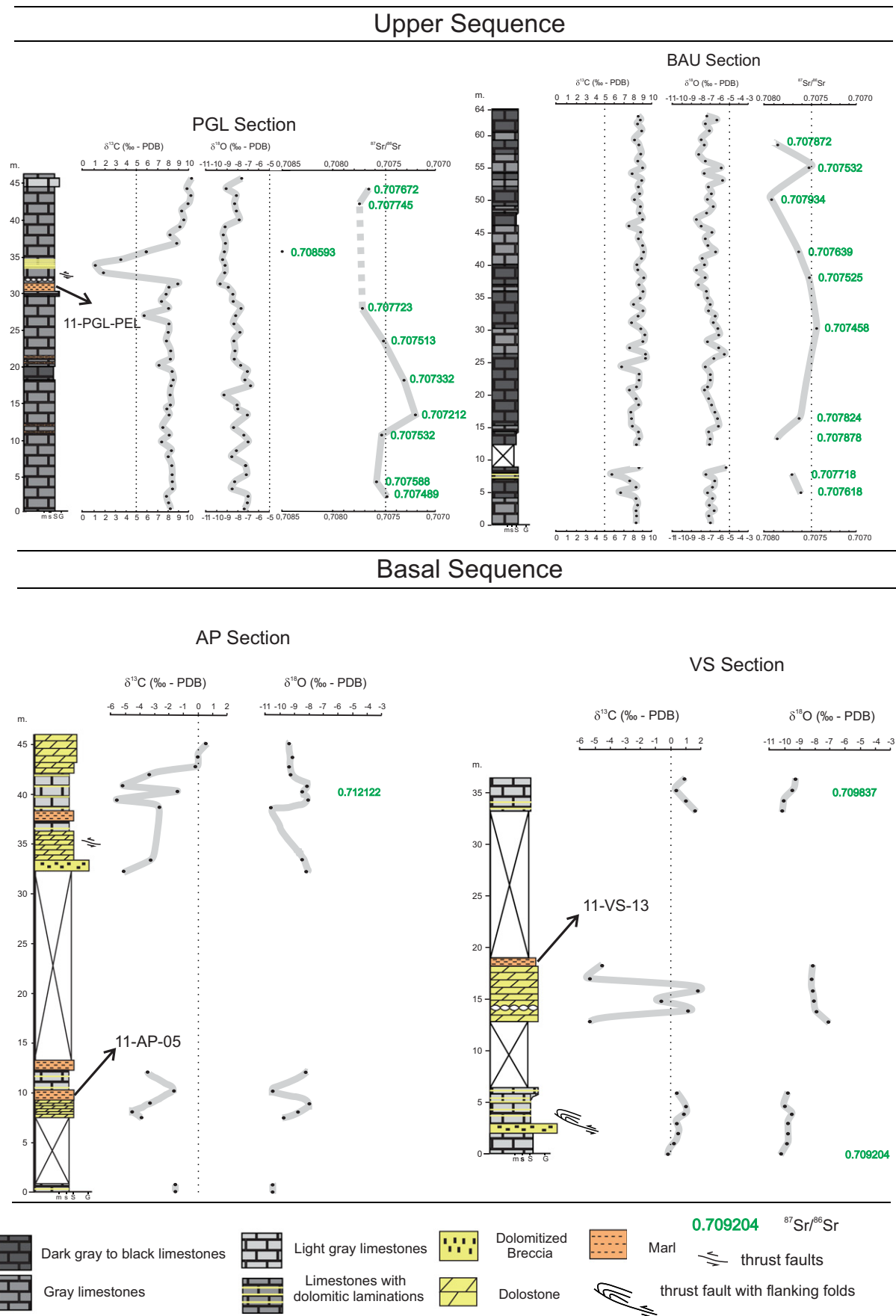
The recently published Sr and Ca isotope data of the carbonates of the Sete Lagoas Formation led to the same uncertainty. Sr isotope chemostratigraphy has been successfully used to correlate carbonate successions, especially the Neoproterozoic ones that lack reliable biostratigraphic markers (Derry et al., 1992; Misi and Veizer, 1998; Walter et al., 2000; Alvarenga et al., 2004, 2008; Ovchinnikova et al., 2012; Li et al., 2013; Kusnetsov et al., 2013). The correlations are performed comparing the  $^{87}\text{Sr}/^{86}\text{Sr}$  ratios of the least altered seawater precipitated carbonates to reference curves of the secular variations of the  $^{87}\text{Sr}/^{86}\text{Sr}$  composition of ancient oceans (Veizer et al., 1989; Halverson et al., 2007). Such variations occur as three main sources deliver different Sr compositions in different proportions to the ocean, namely: i) the Sr runoff from continental weathering, ii) reworking of ancient carbonates on marine platforms, and iii) hydrothermal alteration of the oceanic crust (Palmer and Edmond, 1989). As the Sr residence time in oceans (~2.4 Ma; Jones and Jenkyns, 2001) is considerably higher than the ocean's mixing time ( $10^5$  years; Jacobsen and Kaufman, 1999),  $^{87}\text{Sr}/^{86}\text{Sr}$  ratios of coeval marine carbonates are similar owing to the homogeneity of the Sr isotopic composition for a global ocean and

marginal seas (Kusnetsov et al., 2012). Therefore, Sr chemostratigraphy may be useful for “blind dating” carbonate successions, as long as some caution is taken (Melezik et al., 2001). But the effectiveness of the technique depends on the accuracy of the used reference curve, which is limited due to difficulties to obtain absolute ages on carbonate successions. Moreover, the same  $^{87}\text{Sr}/^{86}\text{Sr}$  ratio can be representative of

different periods in the ocean isotopic evolution. That seems to be the case in the Bambuí Group.  $^{87}\text{Sr}/^{86}\text{Sr}$  ratios around 0.7074–0.7075 are commonly reported for the Sete Lagoas Formation (Babinski et al., 2007; Misi et al., 2007; Kuchenbecker, 2011). Although Caxito et al. (2012) considered these ratios typical of post-Marinoan carbonates by using the Sr evolution curve of Halverson et al. (2010), the same ratios



**Fig. 2.** Geological map of the studied area with the location of the described sections. Modified from Projeto VIDA (2003).

**Fig. 3.** C, O and Sr isotope profiles of the studied sections.

would represent a large interval between 750 and 600 Ma using other compilations as reference (e.g., Jacobsen and Kaufman, 1999; Kusnetsov et al., 2013). It is worth mentioning that some observed sedimentary features common in cap carbonates of distinct ages, such as aragonite pseudomorphs, have been also considered as “typical” of post-Marinoan cap carbonates (Caxito et al., 2012).

On the other hand,  $\delta^{44}\text{Ca}$  trends reported for the cap carbonates of the Sete Lagoas Formation (Silva-Tamayo et al., 2010) are quite similar to those of the Twyitya Formation, a post-Sturtian carbonate succession of NW Canada. Such trends are characterized by a negative excursion immediately in the basal cap carbonates, whereas post-Marinoan successions display such negative excursion higher-up in the sections as a result of initial dissolution of ancient carbonates enriched in  $^{44}\text{Ca}$  that were not available on the aftermath of the Sturtian glaciation (Silva-Tamayo et al., 2010). After the older glacial event, siliciclastic rocks were preferentially weathered during the fallback of the ice sheet, delivering a large amount of  $^{40}\text{Ca}$  into the oceans that resulted in an initial negative excursion.

In this scenario, we present new geochronological (U–Pb, Sm–Nd) and isotope chemostratigraphic (C, O, Sr) data obtained, respectively, on marls and carbonates of the Sete Lagoas Formation. The purpose of this work is to constrain ages for both sequences of the Sete Lagoas Formation on the eastern portion of the basin and to test the efficiency of Sr isotopes on correlating the Bambuí Group to other Neoproterozoic carbonate–siliciclastic successions.

## 2. Geological setting and studied sections

The São Francisco craton sedimentary covers extend for more than 300,000 km<sup>2</sup> (Fig. 1), whereas the Archaean–Palaeoproterozoic basement is mainly exposed in the southern tip and northeast sector of the cratonic region (Teixeira et al., 2000; Alkmin and Martins-Neto, 2012).

The Neoproterozoic cratonic cover comprises, at the base, sparse glacial deposits (e.g., Jequitáí and Carrancas formations), most of them of continental nature, and the marine carbonate–siliciclastic sequences of the Bambuí Group (Rocha-Campos and Hasui, 1981; Karfunkel and

Hoppe, 1988; Martins-Neto and Hercos, 2002; Vieira et al., 2007; Alkmin and Martins-Neto, 2012; Kuchenbecker et al., 2013). Despite tectonic discontinuities (e.g., thrust faults along craton limits), the Neoproterozoic glaciogenic cover has equivalents in both the Araçuaí and Brasília belts, represented by units of the Macaúbas and Ibiá groups, respectively (Uhlein et al., 1999; Dardenne, 2000; Martins-Neto et al., 2001; Pedrosa-Soares et al., 2011a; Babinski et al., 2012).

The Bambuí Group records deposition related to a marine transgression and flexural subsidence of the São Francisco craton, owing to the overload caused by the Brasília and Araçuaí belts’ thrust onto cratonic borders (Martins-Neto et al., 2001; Alkmin and Martins-Neto, 2012). In fact, this group is bounded by thrusts along the edges of the São Francisco craton (Fig. 1). At least in the Araçuaí belt, the carbonate–pelite succession typical of the Bambuí Group has not been found (Pedrosa-Soares et al., 2008, 2011a; Babinski et al., 2012).

In the study region, located close to the southeast thrust boundary between the São Francisco craton and the Araçuaí belt (Fig. 1), the Bambuí Group sharply overlies the Archaean–Palaeoproterozoic basement and is separated from the basement by a shear zone, which is marked by well-developed foliation and stretching lineations, owing to the oriented recrystallization of calcite, mica and chlorite. Deformation and low grade metamorphic recrystallization are more intense in rocks with a pelitic matrix, like marls and carbonates rich in pelitic laminae. This shear zone may show mineral recrystallization assisted by hydrothermal activity, forming sulphides, epidote and other minerals. Well-preserved carbonate layers are found between shear zones, and far from the boundary thrust zone.

According to Dardenne (1978), the Bambuí Group can be subdivided into five units, from base to top (Fig. 1): (i) the Sete Lagoas Formation, composed of limestones and dolomites with interbedded pelitic rock layers (thickness  $\leq 500$  m); (ii) the Serra de Santa Helena Formation, mainly composed of shales and siltstones with interbedded limestones and sandstones (640 m); (iii) the Lagoa do Jacaré Formation, which comprises limestones, siltstones and marbles (350 m); (iv) the Serra da Saudade Formation, constituted of siltstones, green shales and a few limestone

**Table 1**

Major element contents of the analysed carbonates.

	Sample	m.	Si	Al	Mn	Mg	Ca	Na	K	Ti	P	Fe
AP section	11-AP-01	0.0	n.a.	n.a.	n.a.	n.a.	n.a.	n.a.	n.a.	n.a.	n.a.	n.a.
	11-AP-06	10.3	n.a.	n.a.	n.a.	n.a.	n.a.	n.a.	n.a.	n.a.	n.a.	n.a.
VS section	11-AP-14	38.3	n.a.	n.a.	n.a.	n.a.	n.a.	n.a.	n.a.	n.a.	n.a.	n.a.
	11-VS-01	0.0	n.a.	n.a.	n.a.	n.a.	n.a.	n.a.	n.a.	n.a.	n.a.	n.a.
	11-VS-06	4.6	n.a.	n.a.	n.a.	n.a.	n.a.	n.a.	n.a.	n.a.	n.a.	n.a.
	11-VS-07	5.8	n.a.	n.a.	n.a.	n.a.	n.a.	n.a.	n.a.	n.a.	n.a.	n.a.
	11-VS-14	33.2	n.a.	n.a.	n.a.	n.a.	n.a.	n.a.	n.a.	n.a.	n.a.	n.a.
BAU section	11-VS-16	35.2	n.a.	n.a.	n.a.	n.a.	n.a.	n.a.	n.a.	n.a.	n.a.	n.a.
	11-BAU-06	5.0	0.72	0.13	<0.01	0.22	38.66	<0.01	0.04	0.03	0.09	0.17
	11-BAU-09	7.8	0.69	0.13	0.01	0.24	39.05	0.02	0.07	0.03	0.09	0.19
	11-BAU-12	13.3	0.29	0.05	0.01	0.20	39.32	0.01	0.04	0.02	0.05	0.13
	11-BAU-15	16.4	0.17	0.02	0.01	0.19	39.62	0.01	0.02	0.02	0.04	0.11
PGL section	11-BAU-18	19.5	0.89	0.03	0.01	0.20	38.95	<0.01	0.02	0.02	0.05	0.11
	11-BAU-29	30.2	0.24	0.03	0.01	0.24	39.52	0.01	0.01	0.00	0.03	0.00
	11-BAU-37	38.1	0.68	0.17	0.00	0.23	38.55	<0.01	0.10	0.03	0.04	0.19
	11-BAU-41	42.1	0.20	0.03	0.02	0.18	39.78	<0.01	0.02	0.02	0.04	0.15
	11-BAU-49	50.1	0.26	0.06	0.02	0.21	39.42	<0.01	0.04	0.02	0.07	0.15
PGL section	11-BAU-54	55.0	0.14	0.01	0.01	0.11	39.62	<0.01	0.00	0.02	0.04	0.11
	11-BAU-57	58.3	0.11	0.02	0.02	0.22	39.08	0.01	0.02	0.02	0.03	0.13
	11-PGL-03	2.0	0.22	0.04	0.02	0.15	39.65	<0.01	0.02	0.02	0.06	0.13
	11-PGL-05	4.0	0.56	0.13	0.02	0.20	38.87	<0.01	0.07	0.03	0.06	0.20
	11-PGL-11	10.4	0.59	0.12	0.02	0.22	38.98	<0.01	0.03	0.02	0.05	0.19
PGL section	11-PGL-13	12.9	0.58	0.13	0.02	0.17	38.84	<0.01	0.07	0.03	0.05	0.18
	11-PGL-18	17.9	0.81	0.18	0.02	0.21	38.49	<0.01	0.10	0.03	0.05	0.24
	11-PGL-23	23.2	1.78	0.26	0.02	0.22	37.49	<0.01	0.16	0.04	0.07	0.21
	11-PGL-27	27.6	0.19	0.04	0.02	0.17	39.39	0.02	0.02	0.02	0.04	0.14
	11-PGL-33	33.6	4.71	0.94	0.02	2.01	31.37	<0.01	0.62	0.08	0.04	0.77
PGL section	11-PGL-35	35.6	0.34	0.07	0.02	0.14	39.12	0.04	0.04	0.02	0.07	0.20
	11-PGL-41	42.0	0.37	0.11	0.02	0.17	38.87	0.02	0.07	0.03	0.06	0.15
	11-PGL-43	44.1	0.97	0.23	0.02	0.22	37.99	0.02	0.12	0.04	0.06	0.24

Notes: n.a. = not analysed.

**Table 2**Rb and Sr contents, geochemical ratios, C and O isotope values and  $^{87}\text{Sr}/^{86}\text{Sr}$  ratios obtained on analysed carbonates.

	Sample	m.	Rb (ppm)	Sr (ppm)	Mg/Ca	Rb/Sr	Mn/Sr	Fe/Sr	Ca/Sr	$\delta^{13}\text{C} (\text{\textperthousand})$	$\delta^{18}\text{O} (\text{\textperthousand})$	$^{87}\text{Sr}/^{86}\text{Sr}$	error (2 $\sigma$ )
Ana Paula section	11-AP-01	0.0	27	311	—	0.087	—	—	—	-1.6	-10.5	n.a.	n.a.
	11-AP-02	0.9	—	—	—	—	—	—	—	-1.6	-10.5	n.a.	n.a.
	11-AP-03	7.5	—	—	—	—	—	—	—	-3.9	-9.8	n.a.	n.a.
	11-AP-04	8.3	—	—	—	—	—	—	—	-4.6	-8.8	n.a.	n.a.
	11-AP-05	9.3	—	—	—	—	—	—	—	-3.3	-8.0	n.a.	n.a.
	11-AP-06	10.3	28	367	—	0.076	—	—	—	-1.8	-10.5	n.a.	n.a.
	11-AP-07	12.3	—	—	—	—	—	—	—	-3.5	-8.3	n.a.	n.a.
	11-AP-08	32.3	—	—	—	—	—	—	—	-5.1	-8.2	n.a.	n.a.
	11-AP-09	33.4	—	—	—	—	—	—	—	-3.3	-8.5	n.a.	n.a.
	11-AP-10	34.3	—	—	—	—	—	—	<LD	<LD	<LD	n.a.	n.a.
	11-AP-11	35.3	—	—	—	—	—	—	<LD	<LD	<LD	n.a.	n.a.
	11-AP-12	36.3	—	—	—	—	—	—	<LD	<LD	<LD	n.a.	n.a.
	11-AP-14	38.3	21	533	—	0.039	—	—	—	-2.7	-10.7	0.712122	0.000072
	11-AP-15	39.3	—	—	—	—	—	—	—	-5.6	-8.1	n.a.	n.a.
	11-AP-16	40.5	—	—	—	—	—	—	—	-1.4	-8.5	n.a.	n.a.
	11-AP-17	41.5	—	—	—	—	—	—	—	-5.2	-8.2	n.a.	n.a.
	11-AP-18	42.2	—	—	—	—	—	—	—	-3.4	-9.3	n.a.	n.a.
	11-AP-19	43.2	—	—	—	—	—	—	—	-0.2	-9.4	n.a.	n.a.
	11-AP-20	44.2	—	—	—	—	—	—	—	-0.1	-9.2	n.a.	n.a.
	11-AP-21	45.2	—	—	—	—	—	—	—	0.5	-9.4	n.a.	n.a.
Vespasiano section	11-VS-01	0.0	13	532	—	0.025	—	—	—	-0.1	-10.2	0.709204	0.000066
	11-VS-02	1.0	—	—	—	—	—	—	—	0.1	-9.9	n.a.	n.a.
	11-VS-03	2.0	—	—	—	—	—	—	—	0.4	-9.8	n.a.	n.a.
	11-VS-04	2.9	—	—	—	—	—	—	—	0.3	-9.8	n.a.	n.a.
	11-VS-05	3.8	—	—	—	—	—	—	—	0.9	-9.6	n.a.	n.a.
	11-VS-06	4.6	23	373	—	0.063	—	—	—	1.0	-10.0	n.a.	n.a.
	11-VS-07	5.8	27	358	—	0.074	—	—	—	0.3	-9.8	n.a.	n.a.
	11-VS-08	12.8	—	—	—	—	—	—	—	-5.3	-7.1	n.a.	n.a.
	11-VS-09	13.8	—	—	—	—	—	—	—	1.1	-7.9	n.a.	n.a.
	11-VS-10	14.7	—	—	—	—	—	—	—	-0.7	-8.1	n.a.	n.a.
	11-VS-11	15.7	—	—	—	—	—	—	—	1.8	-8.2	n.a.	n.a.
	11-VS-12	17.0	—	—	—	—	—	—	—	-5.3	-8.3	n.a.	n.a.
	11-VS-13	18.3	—	—	—	—	—	—	—	-4.6	-8.2	n.a.	n.a.
	11-VS-14	33.2	27	272	—	0.101	—	—	—	1.6	-10.2	n.a.	n.a.
	11-VS-15	34.2	—	—	—	—	—	—	—	1.0	-10.1	n.a.	n.a.
	11-VS-16	35.2	27	397	—	0.067	—	—	—	0.3	-9.6	0.709837	0.000062
	11-VS-17	36.4	—	—	—	—	—	—	—	0.9	-9.3	n.a.	n.a.
Pedra do Baú section	11-BAU-01	0.4	—	—	—	—	—	—	—	8.2	-7.0	n.a.	n.a.
	11-BAU-02	1.4	—	—	—	—	—	—	—	8.3	-7.2	n.a.	n.a.
	11-BAU-03	2.2	—	—	—	—	—	—	—	8.2	-6.7	n.a.	n.a.
	11-BAU-04	3.1	—	—	—	—	—	—	—	8.4	-7.1	n.a.	n.a.
	11-BAU-05	4.1	—	—	—	—	—	—	—	8.2	-6.8	n.a.	n.a.
	11-BAU-06	5.0	5	2176	0.006	0.002	<0.001	0.804	178	6.7	-7.3	0.707618	0.000054
	11-BAU-07	5.8	—	—	—	—	—	—	—	8.2	-6.8	n.a.	n.a.
	11-BAU-08	6.8	—	—	—	—	—	—	—	7.6	-6.6	n.a.	n.a.
	11-BAU-09	7.8	7	1045	0.006	0.007	0.074	1.807	374	5.8	-7.5	0.707718	0.000063
	11-BAU-10	8.8	—	—	—	—	—	—	—	8.6	-5.3	n.a.	n.a.
	11-BAU-11	12.3	—	—	—	—	—	—	—	8.3	-7.1	n.a.	n.a.
	11-BAU-12	13.3	5	1830	0.005	0.003	0.042	0.688	215	8.6	-7.0	0.707878	0.000050
	11-BAU-13	14.3	—	—	—	—	—	—	—	8.5	-7.2	n.a.	n.a.
	11-BAU-14	15.3	—	—	—	—	—	—	—	7.9	-6.1	n.a.	n.a.
	11-BAU-15	16.4	4	1406	0.005	0.003	0.055	0.796	282	7.8	-6.2	0.707824	0.000050
	11-BAU-16	17.4	—	—	—	—	—	—	—	7.7	-6.5	n.a.	n.a.
	11-BAU-17	18.5	—	—	—	—	—	—	—	8.5	-6.9	n.a.	n.a.
	11-BAU-18	19.5	4	1546	0.005	0.002	0.050	0.724	252	8.3	-7.1	0.707636	0.000056
	11-BAU-19	20.8	—	—	—	—	—	—	—	7.6	-7.7	n.a.	n.a.
	11-BAU-20	21.3	—	—	—	—	—	—	—	8.2	-7.3	n.a.	n.a.
	11-BAU-21	22.3	—	—	—	—	—	—	—	8.6	-7.0	n.a.	n.a.
	11-BAU-22	23.3	—	—	—	—	—	—	—	8.6	-7.0	n.a.	n.a.
	11-BAU-23	24.4	—	—	—	—	—	—	—	6.8	-7.6	n.a.	n.a.
	11-BAU-24	25.5	—	—	—	—	—	—	—	9.3	-6.7	n.a.	n.a.
	11-BAU-25	26.3	—	—	—	—	—	—	—	9.3	-5.6	n.a.	n.a.
	11-BAU-26	27.3	—	—	—	—	—	—	—	7.6	-6.1	n.a.	n.a.
	11-BAU-27	28.3	—	—	—	—	—	—	—	9.0	-7.3	n.a.	n.a.
	11-BAU-28	29.3	—	—	—	—	—	—	—	9.2	-6.1	n.a.	n.a.
	11-BAU-29	30.2	4	1885	0.006	0.002	0.041	<0.001	210	8.8	-6.2	0.707458	0.000059
	11-BAU-30	31.2	—	—	—	—	—	—	—	7.8	-6.7	n.a.	n.a.
	11-BAU-31	32.2	—	—	—	—	—	—	—	8.5	-6.5	n.a.	n.a.
	11-BAU-32	33.0	—	—	—	—	—	—	—	9.0	-7.2	n.a.	n.a.
	11-BAU-33	34.0	—	—	—	—	—	—	—	8.0	-7.0	n.a.	n.a.
	11-BAU-34	35.0	—	—	—	—	—	—	—	8.8	-7.3	n.a.	n.a.
	11-BAU-35	36.0	—	—	—	—	—	—	—	9.0	-7.4	n.a.	n.a.
	11-BAU-36	37.0	—	—	—	—	—	—	—	8.6	-8.3	n.a.	n.a.
	11-BAU-37	38.1	7	2160	0.006	0.003	<0.001	0.874	178	9.1	-7.6	0.707525	0.000059
	11-BAU-38	39.3	—	—	—	—	—	—	—	8.4	-8.5	n.a.	n.a.

(continued on next page)

**Table 2** (continued)

	Sample	m.	Rb (ppm)	Sr (ppm)	Mg/Ca	Rb/Sr	Mn/Sr	Fe/Sr	Ca/Sr	$\delta^{13}\text{C}$ (‰)	$\delta^{18}\text{O}$ (‰)	$^{87}\text{Sr}/^{86}\text{Sr}$	error (2 $\sigma$ )	
Pedra do Baú section	11-BAU-39	40.1	–	–	–	–	–	–	8.3	–7.7	n.a.	n.a.		
	11-BAU-41	42.1	3	1720	0.005	0.002	0.090	0.854	231	9.1	–6.4	0.707639	0.000055	
	11-BAU-42	43.1	–	–	–	–	–	–	9.0	–7.2	n.a.	n.a.		
	11-BAU-43	44.1	–	–	–	–	–	–	8.5	–7.6	n.a.	n.a.		
	11-BAU-44	45.1	–	–	–	–	–	–	8.8	–6.9	n.a.	n.a.		
	11-BAU-45	46.1	–	–	–	–	–	–	7.5	–8.0	n.a.	n.a.		
	11-BAU-46	47.1	–	–	–	–	–	–	9.0	–8.5	n.a.	n.a.		
	11-BAU-47	48.1	–	–	–	–	–	–	8.7	–7.4	n.a.	n.a.		
	11-BAU-48	49.1	–	–	–	–	–	–	8.8	–6.7	n.a.	n.a.		
	11-BAU-49	50.1	4	1809	0.005	0.002	0.086	0.851	218	8.1	–7.3	0.707934	0.000049	
	11-BAU-50	51.1	–	–	–	–	–	–	8.7	–6.9	n.a.	n.a.		
	11-BAU-51	52.1	–	–	–	–	–	–	8.5	–7.2	n.a.	n.a.		
	11-BAU-52	53.1	–	–	–	–	–	–	8.9	–5.7	n.a.	n.a.		
	11-BAU-53	54.1	–	–	–	–	–	–	7.9	–7.7	n.a.	n.a.		
	11-BAU-54	55.0	3	1045	0.003	0.003	0.074	1.071	379	9.0	–5.8	0.707532	0.000072	
	11-BAU-55	56.1	–	–	–	–	–	–	8.4	–7.6	n.a.	n.a.		
	11-BAU-56	57.1	–	–	–	–	–	–	8.8	–8.2	n.a.	n.a.		
	11-BAU-57	58.3	4	1929	0.006	0.002	0.120	0.689	203	8.6	–7.7	0.707872	0.000054	
	11-BAU-58	59.2	–	–	–	–	–	–	8.1	–8.0	n.a.	n.a.		
	11-BAU-59	60.4	–	–	–	–	–	–	8.9	–7.1	n.a.	n.a.		
	11-BAU-60	61.4	–	–	–	–	–	–	8.4	–7.6	n.a.	n.a.		
	11-BAU-61	62.4	–	–	–	–	–	–	8.8	–6.3	n.a.	n.a.		
	11-BAU-62	63.0	–	–	–	–	–	–	8.5	–7.4	n.a.	n.a.		
Parque da Gruta da Lapinha section	11-PGL-01	0.0	–	–	–	–	–	–	8.2	–7.4	n.a.	n.a.		
	11-PGL-02	1.0	–	–	–	–	–	–	8.1	–7.1	n.a.	n.a.		
	11-PGL-03	2.0	2	2563	0.004	0.001	0.060	0.519	155	7.9	–7.1	0.707489	0.000064	
	11-PGL-04	3.0	–	–	–	–	–	–	8.4	–8.5	n.a.	n.a.		
	11-PGL-05	4.0	3	2755	0.005	0.001	0.056	0.711	141	8.4	–8.3	0.707588	0.000066	
	11-PGL-06	5.0	–	–	–	–	–	–	8.4	–7.2	n.a.	n.a.		
	11-PGL-07	6.0	–	–	–	–	–	–	8.3	–7.3	n.a.	n.a.		
	11-PGL-08	7.2	–	–	–	–	–	–	8.0	–8.5	n.a.	n.a.		
	11-PGL-09	8.2	–	–	–	–	–	–	8.3	–8.1	n.a.	n.a.		
	11-PGL-10	9.2	–	–	–	–	–	–	7.4	–7.0	n.a.	n.a.		
	11-PGL-11	10.4	2	2809	0.006	0.001	0.055	0.672	139	8.0	–7.5	0.707532	0.000065	
	11-PGL-12	11.4	–	–	–	–	–	–	7.5	–8.4	n.a.	n.a.		
	11-PGL-13	12.9	4	3393	0.005	0.001	0.046	0.536	114	8.2	–7.1	0.707212	0.000062	
	11-PGL-14	13.9	–	–	–	–	–	–	7.8	–8.0	n.a.	n.a.		
	11-PGL-15	14.9	–	–	–	–	–	–	8.3	–8.1	n.a.	n.a.		
	11-PGL-16	15.9	–	–	–	–	–	–	8.4	–9.3	n.a.	n.a.		
	11-PGL-17	16.9	–	–	–	–	–	–	8.4	–6.8	n.a.	n.a.		
	11-PGL-18	17.9	5	2758	0.005	0.002	0.056	0.862	140	8.5	–7.4	0.707332	0.000075	
	11-PGL-19	18.9	–	–	–	–	–	–	8.4	–7.1	n.a.	n.a.		
	11-PGL-20	19.8	–	–	–	–	–	–	7.2	–7.7	n.a.	n.a.		
	11-PGL-21	20.8	–	–	–	–	–	–	8.2	–8.3	n.a.	n.a.		
	11-PGL-22	21.8	–	–	–	–	–	–	8.2	–8.3	n.a.	n.a.		
	11-PGL-23	23.2	7	3650	0.006	0.002	0.064	0.575	103	7.8	–8.4	0.707513	0.000072	
	11-PGL-24	24.4	–	–	–	–	–	–	8.0	–7.8	n.a.	n.a.		
	11-PGL-25	25.5	–	–	–	–	–	–	8.1	–8.4	n.a.	n.a.		
	11-PGL-26	26.6	–	–	–	–	–	–	5.8	–8.2	n.a.	n.a.		
	11-PGL-27	27.6	3	2260	0.004	0.001	0.069	0.619	174	8.1	–7.7	0.707723	0.000063	
	11-PGL-28	28.6	–	–	–	–	–	–	7.4	–8.5	n.a.	n.a.		
	11-PGL-29	29.6	–	–	–	–	–	–	7.8	–8.5	n.a.	n.a.		
	11-PGL-30	30.1	–	–	–	–	–	–	8.1	–8.9	n.a.	n.a.		
	11-PGL-31	31.6	–	–	–	–	–	–	8.9	–9.7	n.a.	n.a.		
	11-PGL-32	32.6	–	–	–	–	–	–	1.9	–9.3	n.a.	n.a.		
	11-PGL-33	33.6	26	462	0.064	0.057	0.503	16.655	679	1.2	–9.3	n.a.	n.a.	
	11-PGL-34	34.6	–	–	–	–	–	–	3.6	–9.4	n.a.	n.a.		
	11-PGL-35	35.6	3	2704	0.004	0.001	0.086	0.750	145	6.0	–9.3	0.708593	0.000076	
	11-PGL-36	36.6	–	–	–	–	–	–	8.9	–9.2	n.a.	n.a.		
	11-PGL-37	37.8	–	–	–	–	–	–	8.2	–9.3	n.a.	n.a.		
	11-PGL-38	38.8	–	–	–	–	–	–	9.1	–9.2	n.a.	n.a.		
	11-PGL-39	39.8	–	–	–	–	–	–	9.5	–7.9	n.a.	n.a.		
	11-PGL-40	41.0	–	–	–	–	–	–	9.3	–8.1	n.a.	n.a.		
	11-PGL-41	42.0	4	3200	0.005	0.001	0.048	0.481	121	9.9	–8.3	0.707745	0.000062	
	11-PGL-42	43.1	–	–	–	–	–	–	10.2	–8.1	n.a.	n.a.		
	11-PGL-43	44.1	6	2961	0.006	0.002	0.052	0.803	128	9.8	–9.1	0.707672	0.000068	
	11-PGL-44	45.4	–	–	–	–	–	–	10.2	–7.6	n.a.	n.a.		

Notes: – = no data for calculation; n.a. = not analysed.

layers (200 m); and (v) the Três Marias Formation, composed by arkosic sandstones and siltstones. The Bambuí Group records a marine transgression caused by flexural subsidence of the São Francisco Craton, due to the development of the Brasília Belt at the west of the craton (Martins-Neto et al., 2001; Alkmin and Martins-Neto, 2012).

The Sete Lagoas Formation comprises two shallowing-upward sequences, recording two transgressive events (Vieira et al., 2007). Its maximum thickness in the studied area is around 200 m. The basal sequence started with the deposition of seafloor precipitates, which include aragonite pseudomorphs, carbonate mud and cement, characterized by

**Table 3**

Summary of LA-ICPMS U-Pb zircon results for sample 11-AP-05.

Grain spot	Radiogenic ratios						Age (Ma)				% disc
	$^{206}\text{Pb}/^{238}\text{U}$	±	$^{207}\text{Pb}/^{235}\text{U}$	±	$^{207}\text{Pb}/^{206}\text{Pb}$	±	$^{206}\text{Pb}/^{238}\text{U}$	±	$^{207}\text{Pb}/^{206}\text{Pb}$	±	
1.1	0.1004	0.0009	0.8226	0.0133	0.0594	0.0005	617	5	575	18	-7
2.1	0.0980	0.0009	0.8102	0.0131	0.0601	0.0005	603	5	602	18	0
3.1	0.0885	0.0009	0.7157	0.0148	0.0586	0.0009	547	5	544	33	0
4.1	0.0939	0.0009	0.7722	0.0123	0.0594	0.0005	578	5	576	18	0
5.1	0.0962	0.0009	0.7908	0.0124	0.0598	0.0005	592	5	590	18	0
6.1	0.0973	0.0009	0.8052	0.0127	0.0597	0.0005	599	5	585	17	-2
7.1	0.0948	0.0009	0.7755	0.0122	0.0594	0.0005	584	5	576	17	-1
8.1	0.1026	0.0011	0.8722	0.0151	0.0609	0.0005	630	6	631	18	0
9.1	0.0654	0.0008	0.5038	0.0101	0.0551	0.0006	408	5	410	22	0
10.1	0.0965	0.0009	0.7952	0.0125	0.0599	0.0005	594	5	593	18	0
11.1	0.0972	0.0009	0.8060	0.0126	0.0600	0.0005	598	5	596	18	0
12.1	0.0970	0.0009	0.8016	0.0124	0.0596	0.0005	597	5	582	17	-2
13.1	0.0959	0.0009	0.7873	0.0121	0.0597	0.0005	591	5	588	17	0

Notes: Errors are 1-sigma.

$\delta^{13}\text{C}$  values as low as  $-4.5\text{\textperthousand}$ . These isotopic and sedimentary features are typical of other cap carbonates found elsewhere in the globe (Grotzinger and Knoll, 1995; Kennedy, 1996; Hoffman and Schrag, 2002). These deposits are overlain by low organic matter content carbonates with  $\delta^{13}\text{C}$  values around  $0\text{\textperthousand}$ . After a basin drowning, the second sequence started with abundant pelitic deposits immediately overlain by organic-rich black carbonates with  $\delta^{13}\text{C}$  values around  $+8\text{\textperthousand}$ . This abrupt shift in Sete Lagoas Formation C isotopes is a basinal stratigraphic marker (Santos et al., 2000; Kuchenbecker, 2011). The  $\delta^{13}\text{C}$  values keep increasing upwards, reaching values as high as  $+14\text{\textperthousand}$  in stromatolitic carbonates just below the Serra de Santa Helena Formation (Iyer et al., 1995; Vieira et al., 2007).

### 2.1. Studied area and sections

The studied area is located at the central portion of Minas Gerais State, Brazil, between Lagoa Santa and Vespasiano cities (Fig. 2). The Bambuí Group unconformably overlies migmatites and gneisses of the São Francisco Craton basement exposed to the south of the area. Both lower and upper sequences of the Sete Lagoas Formation crop out in the study area. The lower sequence directly overlies the basement on the southeast and also outcrops in a N-S segment that extends from Confins airport to the north of the area. The upper sequence crops out mainly at the northwest of Lagoa Santa City. An occurrence of the Carrancas Conglomerate is found nearby São José da Lapa City (Vieira et al., 2007). The Serra de Santa Helena deposits crop out around the Confins airport, the Lagoa Santa lake and to the northeast.

Two sections from the basal sequence (Vespasiano – VS, Ana Paula – AP) and two sections from the upper sequence (Pedra do Baú – BAU, Gruta da Lapinha Park – PGL) were described and sampled (Fig. 2). Although rocks from all sections display mineral recrystallization features, sedimentary structures were not completely obliterated.

Sections of the basal sequence comprise mainly light grey limestones and beige dolomites (Fig. 3). Carbonate grains are sand sized. The AP section is 46 m thick and display low-angle truncated lamination as the main sedimentary feature, whereas the VS section is 37 m thick and has plane parallel lamination as the main sedimentary structure. The percentage of siliciclastic sediments within the carbonate matrix ranges between 20 and 30% in the AP section decreasing to 5–7% in the VS section. Marl intercalations (siliciclastic content higher than 60%) were described on both sections and sampled for geochronology (Fig. 3). Dolomite occurrences are usually found along to thrust faults with a W-vergence and associated with other tectonic structures (*brecias, boudins*), suggesting dolomitisation during tectonic events.

The upper sequence sections are characterized by massive outcrops of dark grey to black organic-rich limestones (Fig. 3). The carbonate grains are silt/sand sized. The BAU section is 64 m thick and the PGL

section is 46 m thick. Both sections display plane parallel laminations as the main sedimentary structure and scarce low-angle truncated laminations. The percentage of siliciclastic material in the carbonate matrix is lower than 2%. Marl intercalations occur in the PGL section and the thickest one was sampled for geochronology (Fig. 3).

### 3. Materials and methods

Four sections located between the cities of Vespasiano and Lagoa Santa (AP, VS, BAU and PGL; Fig. 2) were described in this study. A number of 143 carbonates and 3 marls were sampled for chemostratigraphy and geochronological analysis, respectively. All isotopic and geochronological analyses were carried out at the Center of Geochronological Research (CPGeo) of University of São Paulo.

Carbonate powders were obtained by microdrilling homogeneous sample areas, whereas fractured, weathered and mineral-filled zones were avoided. C and O analyses were carried out by reacting sample powders with 100%  $\text{H}_3\text{PO}_4$ , under a He atmosphere. The C and O compositions of the  $\text{CO}_2$  extracted were then measured in a Delta Advantage mass spectrometer. The results are reported in the  $\delta$  notation, relative to PDB standard.

Sr isotopic compositions were obtained only in carbonate samples with Sr contents higher than 300 ppm. Compositions were obtained using a two-step leaching technique. First leaching was performed by reacting ~100 mg of sample powders with HCl 0.1 N solution for 1 h. After drying, the samples were centrifuged and washed three times with Milli Q water. These first leachates were discarded. The residues underwent reaction with HCl 1 N solution for 30 min. After drying, the samples were again centrifuged and washed three times with Milli Q water. These second leachates were separated from the residue and purified by the ion exchange chromatography technique. Their  $^{87}\text{Sr}/^{86}\text{Sr}$  ratios were measured on a Finnigan MAT 262 mass spectrometer.  $^{87}\text{Sr}/^{86}\text{Sr}$  ratios were normalized for the value 0.1194, and the average value of the NBS-987 standard measured during analysis was  $0.710251 \pm 0.000043$ .

Rb and Sr contents of carbonate rocks were measured in 10 g of whole rock samples by the X-Ray Fluorescence technique on a Philips PW 2510 X-ray spectrometer at the Fluorescence Laboratory/ICP-OES of USP. Other trace and major contents were determined by melting 0.2 g of whole rock samples with lithium metaborate/tetraborate, followed by diluted nitric acid attack and ICP-OES analysis at Acme Laboratory (Canada).

U-Pb ages were obtained on detrital zircons retrieved from marl sample matrix. The acquisition of the isotopic data was performed using a NEPTUNE-ICP-MS coupled with a laser ablation system. To normalize the  $^{207}\text{Pb}/^{206}\text{Pb}$  ratio the NIST 612 and external standards were used, while the  $^{206}\text{Pb}/^{238}\text{U}$  ratio was normalized by external standards. For mass bias correction the GJ standard (600 Ma; Elhlou et al., 2006) was used.

## 4. Results

### 4.1. Carbonate geochemistry

The major element contents of each sample are shown in Table 1 and the Rb and Sr contents, Mg/Ca, Rb/Sr, Mn/Sr, Fe/Sr and Ca/Sr ratios and isotopic results are presented in Table 2.

Carbonates from the basal sequence are characterized by low Sr (<550 ppm) and high Rb contents (>10 ppm), as well as Rb/Sr ratios ranging in the 0.02–0.10 interval. Therefore, only three samples were analysed for Sr isotopes, 11-AP-14, 11-VS-01 and 11-VS-13. The measured  $^{87}\text{Sr}/^{86}\text{Sr}$  ratios are very radiogenic:  $0.712122 \pm 0.000072$ ,  $0.709204 \pm 0.000066$  and  $0.709840 \pm 0.000062$ , respectively. The  $\delta^{13}\text{C}$  values obtained on samples from the AP section range between  $-5.6$  and  $0.5\text{\textperthousand}$  (Table 2). No defined trend is observed from base to top and the samples display a large variation throughout stratigraphy. Consistent values are found only at the base ( $-1.6\text{\textperthousand}$ ) and at the three uppermost samples ( $\delta^{13}\text{C}$  values between  $-0.2$  and  $+0.5\text{\textperthousand}$ ).  $\delta^{18}\text{O}$  values from the AP section range from  $-10.7$  to  $-8\text{\textperthousand}$  and have a similar behaviour to that shown in the C isotope values, although not so heterogeneous. Carbonates from the basal and upper portions of the VS section yielded  $\delta^{13}\text{C}$  values between  $-0.1$  and  $+1.6\text{\textperthousand}$  (Table 2), with a general upward increasing trend. Dolostones from the central portion yielded  $\delta^{13}\text{C}$  values ranging from  $-5.3$  to  $+1.8\text{\textperthousand}$  with a large variation among adjacent samples. The  $\delta^{18}\text{O}$  values obtained on basal and upper portion samples vary between  $-10.2$  and  $-9.3\text{\textperthousand}$  and those obtained on central portion samples vary from  $-8.3$  to  $-7.1\text{\textperthousand}$ .

Carbonates from the upper sequence displayed high Sr (>1000 ppm) and low Rb contents (<10 ppm), as well as Rb/Sr ratios lower than 0.01 (Table 2). As petrography revealed that these rocks are more homogeneous than those from basal sequence and almost free from siliciclastic sediments on matrix admixture, further geochemical analyses were performed. Samples showed low Fe and Mn contents (<0.01–0.29% and <0.01–0.03%, respectively), and low Mg content (0.11–0.26%) compared to Ca (37.49–39.78%). The resulting Mn/Sr, Fe/Sr, Ca/Sr and Mg/Ca ratios are lower than 0.12, 1.10, 380 and 0.01, respectively (Table 2). These data suggested that the samples were ideal for Sr isotope analyses. The BAU section carbonates showed  $^{87}\text{Sr}/^{86}\text{Sr}$  ratios ranging from  $0.707458 \pm 0.000059$  to  $0.707934 \pm 0.000049$  and the Sr richest limestone (2176 ppm – sample 11-BAU-06) has a ratio of  $0.707618 \pm 0.000054$ .  $^{87}\text{Sr}/^{86}\text{Sr}$  ratios of the PGL carbonates range from  $0.707212 \pm 0.000062$  to  $0.707745 \pm 0.000062$  and the Sr richest sample (3650 ppm – sample 11-PGL-23) presented a ratio of  $0.707513 \pm 0.000072$ . Sample 11-PGL-33 is out of these ranges. It has lower Sr content (462 ppm) and higher Rb content (26 ppm – Table 2) attached to an increase on the Mg content (Table 1) and was obtained from a partially dolomitised layer. The obtained  $^{87}\text{Sr}/^{86}\text{Sr}$  ratio was  $0.708593 \pm 0.000076$ .

Samples from the BAU section presented  $\delta^{13}\text{C}$  values between  $+5.8$  and  $+9.3\text{\textperthousand}$  (Table 2). Sample 11-BAU-09 displayed the lowest value ( $+5.8\text{\textperthousand}$ ) and contained some millimetric dolomite laminations. The  $\delta^{18}\text{O}$  values obtained vary between  $-8.5$  and  $-5.3\text{\textperthousand}$ .  $\delta^{13}\text{C}$  values obtained on carbonate samples from the PGL section range from  $+1.2$  to  $+10.2\text{\textperthousand}$ . Despite the wide interval, almost all samples present values higher than  $+7\text{\textperthousand}$ . The lower values were obtained on carbonates collected between the 32–36 m interval that display millimetric dolomite laminations associated with a small thrust fault. The  $\delta^{18}\text{O}$  values obtained vary between  $-9.7$  and  $-6.8\text{\textperthousand}$ .

### 4.2. Geochronological data

Three layers of marl were sampled for geochronological analysis. The U–Pb data is presented in Tables 3, 4 and 5 (AP, VS and PGL, respectively). Their stratigraphic position on sections AP, VS and PGL is shown in Fig. 3.

Only 13 zircon grains were retrieved from sample 11-AP-05 and their size range from 80 to 400  $\mu\text{m}$ . Most of the zircons are prismatic and do not show igneous oscillatory zoning (Fig. 4). The concordant

$^{206}\text{Pb}/^{238}\text{U}$  ages obtained are in the 547–630 Ma interval (Fig. 5). About 77% of the grains show ages between 560 and 620 Ma and a concordia age of  $592.9 \pm 1.7$  Ma was obtained (Fig. 5).

Sample 11-VS-13 provided 77 zircon grains, which are mainly prismatic and round shaped and their size is no longer than 80  $\mu\text{m}$  (Fig. 4). Most of the grains show igneous oscillatory zoning on cathodoluminescence images. The two most important zircon populations (~65% of the grains) show peaks at 967 and 1068 (Figs. 5 and 6). Other important populations are 873 and 934 Ma (6%), 1100 Ma (4%) and 1271 Ma (3%). There are also Palaeoproterozoic grains and an Archaean crystal dated at 3.68 Ga.

Seventy seven zircon grains were recovered from sample 11-PGL-PEL. They are mainly prismatic and their size is no longer than 70  $\mu\text{m}$ . The cathodoluminescence images reveal igneous oscillatory zoning (Fig. 4). The U–Pb ages indicate three important Neoproterozoic populations at ~625 (63% of the grains), ~579 and ~557 Ma (26% of the grains – Fig. 6).

## 5. Discussion

### 5.1. Isotope chemostratigraphy

The isotope chemostratigraphy is considered a powerful tool for correlating carbonate successions worldwide, especially the Proterozoic ones that lack robust fossil record (Jacobsen and Kaufman, 1999; Hoffman and Schrag, 2002; Halverson et al., 2010; Kusnetsov et al., 2013). But the effectiveness of the technique depends on the reliability of the acquired data and their representativeness regarding the isotope composition of the depositional environment (Melezhik et al., 2001; Frimmel, 2010; Kusnetsov et al., 2013). Therefore, it becomes necessary to evaluate whether the isotope record found within the studied sections of the Sete Lagoas Formation is original or modified by post-depositional events.

Section AP, the central portion of section VS and a carbonate layer from the top of the PGL section display a large oscillation on  $\delta^{13}\text{C}$  values when adjacent samples are compared. The lack of consistency strongly suggests post-depositional alteration of the C isotopic values. Carbonate rocks of those sectors are dolomitised or partially dolomitised (Fig. 3). Such dolomites are linked to tectonic structures, such as thrust faults, breccias and boudins, suggesting a tectonic induced dolomitisation. The large variation on  $\delta^{13}\text{C}$  values requires that a C enriched fluid interacted with the Sete Lagoas Formation carbonates, something not usual to in early diagenetic fluids (Brand and Veizer, 1980; Veizer et al., 1983). Moreover,  $\delta^{13}\text{C}$  vs.  $\delta^{18}\text{O}$  plots show no positive correlation between C and O isotopes and Sr/Ca vs. Mn plots indicate no incorporation of Mn during post-depositional modification (Fig. 7). Both would be expected on a carbonate/diagenetic fluid interaction (Brand and Veizer, 1980; Veizer et al., 1983; Fölling and Frimmel, 2002; Derry, 2010). We therefore conclude that the  $\delta^{13}\text{C}$  values of these sectors are not original, early diagenetic, but were modified during tectonic dolomitisation.

The rest of the studied sections display consistent  $\delta^{13}\text{C}$  values that are considered primary and represent the original depositional marine environment. The C isotope curve of the Sete Lagoas Formation is quite similar along all the São Francisco Craton and the abrupt shift from  $\delta^{13}\text{C}$  values around  $0\text{\textperthousand}$  at the basal sequence to values higher than  $8\text{\textperthousand}$  on the upper sequence is a regional stratigraphical mark (Santos et al., 2000). The best preserved values from  $-1.6\text{\textperthousand}$  to slightly positive ones for sections AP and VS confirm their stratigraphic position on the basal sequence proposed by our field and petrographic observations. Also, the absence of an expressive negative C excursion indicates that such sections are above the basal cap carbonates. The highly positive values obtained for sections PGL and BAU also confirm that they belong to the upper sequence as pointed out by field descriptions.

Unlike  $\delta^{13}\text{C}$  values, the Sr isotope chemostratigraphy is not a good tool for intrabasinal correlation of the Sete Lagoas Formation sections,

**Table 4**

Summary of LA-ICPMS U-Pb zircon results for sample 11-VS-13.

Grain spot	Radiogenic ratios						Age (Ma)				% disc
	$^{206}\text{Pb}/^{238}\text{U}$	±	$^{207}\text{Pb}/^{235}\text{U}$	±	$^{207}\text{Pb}/^{206}\text{Pb}$	±	$^{206}\text{Pb}/^{238}\text{U}$	±	$^{207}\text{Pb}/^{206}\text{Pb}$	±	
1.1	0.1075	0.0009	0.9158	0.0230	0.0618	0.0014	658	5	661	50	0
2.1	0.3881	0.0034	7.2441	0.1813	0.1355	0.0031	2114	16	2166	38	2
3.1	0.1462	0.0008	1.4485	0.0349	0.0715	0.0016	880	4	972	47	9
4.1	0.1615	0.0011	1.6741	0.0399	0.0744	0.0017	965	6	1054	46	8
5.1	0.1804	0.0005	1.9055	0.0437	0.0768	0.0017	1069	2	1119	45	4
6.1	0.1593	0.0004	1.5556	0.0358	0.0708	0.0016	953	2	951	46	0
7.1	0.1753	0.0006	1.7942	0.0410	0.0741	0.0016	1041	3	1046	45	0
8.1	0.1672	0.0009	1.6732	0.0391	0.0723	0.0016	996	5	994	46	0
9.1	0.1514	0.0034	1.4870	0.0474	0.0712	0.0016	909	19	961	46	5
10.1	0.2030	0.0027	2.2463	0.0556	0.0799	0.0019	1192	14	1197	47	0
11.1	0.3264	0.0010	5.1319	0.1158	0.1140	0.0025	1821	5	1866	38	2
12.1	0.1704	0.0009	1.7038	0.0400	0.0728	0.0016	1014	5	1009	45	0
13.1	0.0868	0.0007	0.7032	0.0177	0.0584	0.0013	537	4	539	48	0
14.1	0.1721	0.0009	1.8197	0.0257	0.0771	0.0009	1024	5	1127	23	9
15.1	0.1625	0.0021	1.6080	0.0322	0.0738	0.0008	970	12	1038	23	6
16.1	0.1823	0.0009	1.9409	0.0276	0.0776	0.0009	1079	5	1139	23	5
17.1	0.1600	0.0008	1.6138	0.0224	0.0729	0.0008	957	4	1012	23	5
18.1	0.1741	0.0011	1.8337	0.0272	0.0787	0.0009	1034	6	1168	22	11
19.1	0.0839	0.0007	0.6741	0.0114	0.0589	0.0008	520	4	555	28	6
20.1	0.1079	0.0009	1.0519	0.0178	0.0705	0.0010	661	5	941	30	30
21.1	0.2249	0.0029	3.1970	0.0695	0.1044	0.0013	1308	15	1709	23	23
22.1	0.1750	0.0009	1.8459	0.0266	0.0770	0.0009	1040	5	1123	23	7
23.1	0.1639	0.0008	1.6113	0.0219	0.0717	0.0008	978	4	978	23	0
24.1	0.7660	0.0047	39.4729	0.5579	0.3750	0.0041	3666	17	3684	-24	0
25.1	0.1628	0.0012	1.6116	0.0234	0.0720	0.0008	972	6	984	23	1
26.1	0.2087	0.0019	2.2944	0.0375	0.0806	0.0009	1222	10	1217	22	0
27.1	0.1797	0.0008	1.8358	0.0245	0.0743	0.0009	1065	4	1050	24	-1
28.1	0.1722	0.0005	1.7669	0.0221	0.0749	0.0009	1024	3	1068	23	4
29.1	0.1530	0.0007	1.4913	0.0204	0.0711	0.0008	917	4	960	24	4
30.1	0.1730	0.0006	1.7854	0.0228	0.0752	0.0009	1029	3	1077	23	4
31.1	0.1796	0.0010	1.8670	0.0255	0.0747	0.0008	1065	6	1063	23	0
32.1	0.3272	0.0013	5.6852	0.0770	0.1275	0.0015	1825	6	2061	20	11
33.1	0.1447	0.0007	1.2975	0.0204	0.0680	0.0009	871	4	867	29	0
34.1	0.3554	0.0016	6.0474	0.0922	0.1238	0.0016	1960	8	2010	22	2
35.1	0.1789	0.0007	1.8763	0.0243	0.0764	0.0009	1061	4	1109	23	4
36.1	0.1549	0.0016	1.5961	0.0276	0.0757	0.0010	928	9	1088	27	15
37.1	0.1422	0.0011	1.4233	0.0205	0.0730	0.0008	857	6	1014	23	15
38.1	0.2151	0.0033	2.4796	0.0574	0.0833	0.0011	1256	17	1282	25	2
39.1	0.1559	0.0004	1.5384	0.0190	0.0717	0.0008	934	2	978	23	4
40.1	0.1700	0.0018	1.7398	0.0351	0.0742	0.0011	1012	10	1048	31	3
41.1	0.3238	0.0032	5.4235	0.1080	0.1210	0.0018	1808	16	1970	26	8
42.1	0.5761	0.0059	17.0444	0.3426	0.2147	0.0032	2933	24	2947	24	0
43.1	0.1759	0.0018	1.7682	0.0357	0.0730	0.0011	1045	10	1014	31	-3
44.1	0.1615	0.0016	1.6174	0.0323	0.0728	0.0011	965	9	1009	31	4
45.1	0.1783	0.0025	1.8221	0.0405	0.0745	0.0011	1057	14	1055	30	0
45.2	0.1820	0.0019	1.8952	0.0379	0.0751	0.0011	1078	10	1074	30	0
46.1	0.1671	0.0017	1.6608	0.0328	0.0723	0.0011	996	9	994	31	0
47.1	0.1920	0.0020	2.0667	0.0425	0.0769	0.0012	1132	11	1121	30	-1
48.1	0.1598	0.0020	1.5689	0.0350	0.0711	0.0012	956	11	961	33	0
49.1	0.4788	0.0055	12.0899	0.2518	0.2184	0.0037	2522	24	2975	27	15
50.1	0.1617	0.0016	1.5832	0.0315	0.0715	0.0011	966	9	971	31	0
51.1	0.3341	0.0070	5.6617	0.1652	0.1301	0.0033	1858	34	2096	43	11
52.1	0.1632	0.0009	1.6224	0.0202	0.0727	0.0008	974	5	1006	21	3
53.1	0.1680	0.0007	1.6739	0.0194	0.0726	0.0008	1001	4	1002	24	0
54.1	0.3632	0.0014	6.5888	0.0675	0.1313	0.0013	1997	7	2112	17	5
55.1	0.1618	0.0007	1.5953	0.0158	0.0719	0.0007	967	4	982	21	1
56.1	0.5312	0.0031	14.1589	0.1592	0.1895	0.0019	2746	13	2741	16	0
57.1	0.1691	0.0010	1.6975	0.0242	0.0729	0.0010	1007	6	1011	28	0
58.1	0.1846	0.0006	1.9247	0.0197	0.0757	0.0008	1092	3	1088	21	0
59.1	0.1832	0.0010	1.9132	0.0207	0.0756	0.0007	1085	6	1085	20	0
60.1	0.2181	0.0007	2.5069	0.0245	0.0831	0.0008	1272	4	1276	19	0
61.1	0.1674	0.0012	1.6263	0.0204	0.0726	0.0008	998	7	1002	22	0
62.1	0.1760	0.0006	1.7911	0.0176	0.0742	0.0007	1045	3	1048	20	0
63.1	0.1801	0.0011	1.9283	0.0227	0.0786	0.0008	1068	6	1165	20	8
64.1	0.5847	0.0018	16.6729	0.1607	0.2079	0.0020	2968	8	2896	16	-2
65.1	0.1366	0.0014	1.3332	0.0192	0.0725	0.0010	825	8	999	28	17
66.1	0.3541	0.0036	5.8024	0.1014	0.1199	0.0026	1954	17	1954	37	0
67.1	0.1670	0.0014	1.6945	0.0225	0.0735	0.0010	996	8	1027	28	3
68.1	0.4287	0.0095	9.9853	0.5283	0.1978	0.0040	2300	43	2813	33	18
69.1	0.1512	0.0010	1.3984	0.0210	0.0714	0.0010	908	6	969	29	6
70.1	0.1899	0.0010	1.9995	0.0235	0.0768	0.0011	1121	6	1119	28	0
71.1	0.1878	0.0010	1.9366	0.0221	0.0764	0.0011	1109	5	1107	28	0
72.1	0.1596	0.0010	1.5828	0.0188	0.0728	0.0010	955	6	1009	28	5
73.1	0.2414	0.0016	2.9443	0.0360	0.0892	0.0012	1394	9	1414	26	1

(continued on next page)

**Table 4** (continued)

Grain spot	Radiogenic ratios						Age (Ma)				% disc
	$^{206}\text{Pb}/^{238}\text{U}$	±	$^{207}\text{Pb}/^{235}\text{U}$	±	$^{207}\text{Pb}/^{206}\text{Pb}$	±	$^{206}\text{Pb}/^{238}\text{U}$	±	$^{207}\text{Pb}/^{206}\text{Pb}$	±	
74.1	0.4774	0.0038	11.6930	0.1786	0.1824	0.0025	2516	17	2677	23	6
75.1	0.1645	0.0055	1.5571	0.0645	0.0720	0.0028	982	31	986	78	0
76.1	0.1653	0.0010	1.6355	0.0196	0.0722	0.0010	986	5	990	29	0
77.1	0.1617	0.0020	1.6089	0.0294	0.0723	0.0010	966.4	11.2	993.1	28.7	3

Note: Errors are 1-sigma.

because  $^{87}\text{Sr}/^{86}\text{Sr}$  ratios commonly reported for both sequences are homogenous around 0.7075 (Alvarenga et al., 2007; Babinski et al., 2007; Misi et al., 2007; Kuchenbecker, 2011). However, as Sr residence time in oceans far exceeds this environment's water composition homogenization (Jones and Jenkyns, 2001),  $^{87}\text{Sr}/^{86}\text{Sr}$  ratios of coeval marine carbonates are similar to global ocean and marginal seas Sr isotopic composition (Kusnetsov et al., 2012). The less altered  $^{87}\text{Sr}/^{86}\text{Sr}$  ratios of Sete Lagoas Formation could be then used to correlate the unit to other carbonate successions and to constrain its depositional age.

Sr content of carbonate rocks is a fast and reliable way to track samples that have undergone post-depositional modification of its original isotopic composition (Halverson et al., 2007).  $^{87}\text{Sr}/^{86}\text{Sr}$  ratios vs. Sr content plot (Fig. 7) of studied carbonates clearly shows that samples with less than 600 ppm of Sr have the most radiogenic ratios ( $>0.7092$ ; Table 2). That is the case of all analysed samples from basal sequence. Sections VS and AP have several portions of tectonic dolomitised carbonates that seem to have their original Sr composition leached during tectonism with incorporation of radiogenic Sr (Fig. 3). The  $^{87}\text{Sr}/^{86}\text{Sr}$  ratios of such samples are probably not original and therefore will be discarded. Sample 11-PGL-33 from upper sequence also has a distinguishable radiogenic  $^{87}\text{Sr}/^{86}\text{Sr}$  ratio ( $0.708593 \pm 0.000076$ ), but its Sr content is very high (2704 ppm; Table 2). However, a more careful analysis of the Mn/Sr vs. Mg/Ca diagram shows that this sample has an increase of the Mn/Sr ratio linked to an increase of the Mg/Ca ratio (Fig. 7). As the Sr/Ca vs. Mn content diagram does not exhibit any Mn incorporation on the carbonate composition during decreasing of Sr/Ca ratio (Fig. 7) and the sample is directly above the partially dolomitised zone of the PGL section (Fig. 3), we again propose a tectonic fluid presence during alteration. This sample will also be discarded for Sr isotope chemostratigraphy.

All the remaining carbonate samples are from upper sequence sections. They all display Mn/Sr, Fe/Sr, Ca/Sr and Mg/Ca ratios lower than 0.12, 1.10, 380 and 0.01, respectively (Table 2), which suggest samples with original or little modified Sr isotopic record (Veizer et al., 1989; Fölling and Frimmel, 2002; Kusnetsov et al., 2013). Geochemical diagrams also show that these carbonates do not follow any alteration trend (Fig. 7). Their  $^{87}\text{Sr}/^{86}\text{Sr}$  ratios vary between 0.7072 and 0.7079, and the Sr enriched samples of sections BAU and PGL have ratios close to 0.7075–0.7076 (Table 2). These values are in agreement with previously reported  $^{87}\text{Sr}/^{86}\text{Sr}$  ratios of 0.7075 for the Sete Lagoas Formation (Alvarenga et al., 2007; Babinski et al., 2007; Misi et al., 2007; Kuchenbecker, 2011).

Again, trying to constrain an age for the Sete Lagoas Formation based on Sr "blind dating" is a hard task. Depending on the assumed reference curve of Sr isotopic composition of Neoproterozoic seawater, different age intervals could be assumed. If the curve presented by Halverson et al. (2010) is chosen, then a post-Marinoan age is required for the Bambuí Group. However, in other available Sr evolution curves are used (e.g., Jacobsen and Kaufman, 1999; Melezhik et al., 2001; Kusnetsov et al., 2013) then age constraints are only restricted to a large interval between 750 and 600 Ma for the deposition of the Sete Lagoas Formation. It means that this unit could be either post-Sturtian or post-Marinoan and the Sr isotope chemostratigraphy does not help solve the puzzle concerned to the age of the Bambuí Group. Therefore, it is necessary to look up into our geochronological data.

### 5.2. Age constraining and implications for Bambuí Group

Detailed stratigraphic sections from both sequences of the Sete Lagoas Formation help evaluate a possible unconformity inside the unit and estimate its depositional age. The age data point to the Araçuaí orogen as the source of the dated zircon grains, as most of the obtained ages are found in granitic rocks found therein. About 75% of the grains from sample 11-AP-05 presented ages between 630 and 584 Ma (Table 3), resulting in a concordia age of  $593 \pm 1.7$  Ma (Fig. 5). These data suggest that the sources of the grains are the igneous rocks from the G1 supersuite (630–585 Ma; Pedrosa-Soares et al., 2011b) of the Araçuaí Orogen magmatic arc, located to the east of the São Francisco craton (Fig. 1). Minor sources seem to be represented by collisional granites of the Araçuaí orogen, ranging in age from ca. 585 Ma to ca. 545 Ma (Pedrosa-Soares et al., 2011b; Peixoto et al., 2015).

Sample 11-VS-13 showed different sources from section AP, with an important contribution from Mesoproterozoic rocks (Table 4; Fig. 6). Sources in the 1400–1050 Ma interval are unknown in the Araçuaí–West Congo Orogen. Similar populations were found in the Macaúbas Group (Babinski et al., 2012) and in the Espinhaço Supergroup (Valladares et al., 2004; Valeriano et al., 2004; Chemale et al., 2012), both located to the east of the craton, suggesting that this zircon population found in Sete Lagoas Formation could be reworked from these older units. The oldest Tonian (967 Ma) sources are probably the volcanic rocks and granites from Mayumbian and Zadianian Groups and Noqui granites, dated between  $912 \pm 7$  Ma and  $999 \pm 7$  Ma (Tack et al., 2001). The 873 Ma zircons may come from the anorogenic granites of the northeastern Araçuaí orogen, dated at  $875 \pm 9$  Ma (Silva et al., 2008). The source of the ~656 Ma peak may include plagiogranites of the Ribeirão da Folha ophiolite (Queiroga et al., 2007), the youngest intrusions of the Alkaline Province of Bahia State (Teixeira et al., 1997), sources in the magmatic arcs located in Ribeira belt (Tupinambá et al., 2012; Heilbron et al., 2013), and/or recycled sources containing zircon grains from the referred sources.

The geochronology of the upper sequence is represented by sample 11-PGL-PEL (Table 5). The source of the most important zircon population (~625 Ma – almost 70% of the dated grains; Fig. 6) is probably the G1 supersuite of the Araçuaí orogen (Pedrosa-Soares et al., 2011a, 2011b). The other important peak is ~557 Ma (about 27% of the grains) and its source may be the rocks from syn-collisional G2 supersuite. There are minor contributions from Archaean and Palaeoproterozoic sources from the basement of the São Francisco Craton. A few grains show ages younger than 550 Ma that could be related to Pb loss due hydrothermal fluid percolation along detachment shears between the marl layers during tectonism. However, more precise geochronological analyses have to be done in order to confirm the younger ages obtained from a few zircon grains. In any case, the youngest and voluminous (~27% of the dated grains) zircon population of 557 Ma is the best estimate for the maximum depositional age of the Bambuí Group.

Our U–Pb ages have some important implications for the Sete Lagoas Formation and the Bambuí Group, as they are significantly younger than those previously reported in the literature. The 557 Ma zircon population strongly suggests that the sedimentation of most of the Bambuí Group started in late Ediacaran times. The data also refute the hypothesis of a major gap of ~130 Ma between the sequences. The constant  $^{87}\text{Sr}/$

**Table 5**

Summary of SHRIMP U-Pb zircon results for sample 11-PGL-PEL.

Grão, spot	Radiogenic ratios						Age (Ma)				% disc
	$^{206}\text{Pb}/^{238}\text{U}$	±	$^{207}\text{Pb}/^{235}\text{U}$	±	$^{207}\text{Pb}/^{206}\text{Pb}$	±	$^{206}\text{Pb}/^{238}\text{U}$	±	$^{207}\text{Pb}/^{206}\text{Pb}$	±	
GL 1.1	0.1115	0.0012	0.9548	0.0178	0.0623	0.0009	682	7	678	32	0
GL 1.2	0.0880	0.0010	0.7094	0.0163	0.0593	0.0012	543	6	574	42	5
GL 2.1	0.4063	0.0043	7.2757	0.1331	0.1294	0.0019	2087	25	2087	25	-5
GL 3.1	0.0983	0.0010	0.8165	0.0162	0.0603	0.0010	605	6	607	35	0
GL 4.1	0.1037	0.0011	0.8708	0.0186	0.0610	0.0011	636	7	633	38	0
GL 5.1	0.1059	0.0012	0.9000	0.0172	0.0614	0.0010	649	7	649	34	0
GL 6.1	0.1308	0.0016	2.0435	0.0417	0.1139	0.0017	792	9	1864	27	57
GL 7.1	0.0962	0.0010	0.8072	0.0149	0.0608	0.0009	592	6	626	32	5
GL 8.1	0.1007	0.0010	0.8386	0.0159	0.0608	0.0010	618	6	626	34	1
GL 9.1	0.1025	0.0010	0.8560	0.0159	0.0609	0.0009	629	6	630	33	0
GL 10.1	0.1054	0.0011	0.8893	0.0185	0.0624	0.0011	646	6	683	38	5
GL 11.1	0.0989	0.0011	0.8251	0.0193	0.0602	0.0013	608	7	606	45	0
GL 12.1	0.1039	0.0012	0.8769	0.0170	0.0611	0.0009	637	7	637	33	0
1.1	0.1024	0.0009	0.8547	0.0115	0.0607	0.0005	629	5	621	17	-1
2.1	0.1013	0.0009	0.8602	0.0117	0.0613	0.0005	622	5	644	17	3
3.1	0.0911	0.0008	0.7618	0.0107	0.0606	0.0005	562	5	619	19	9
4.1	0.1021	0.0009	0.8583	0.0114	0.0608	0.0005	627	5	624	17	0
5.1	0.1038	0.0009	0.8766	0.0115	0.0609	0.0005	637	5	629	17	-1
6.1	0.1048	0.0009	0.8845	0.0121	0.0612	0.0005	642	5	641	17	0
7.1	0.1027	0.0009	0.8576	0.0118	0.0610	0.0005	630	5	633	19	0
8.1	0.5868	0.0065	21.6644	0.4656	0.2742	0.0041	3325	23	3325	23	10
9.1	0.1022	0.0010	0.8652	0.0118	0.0608	0.0005	627	6	625	17	0
10.1	0.0924	0.0008	0.7646	0.0108	0.0600	0.0006	570	5	596	20	4
11.1	0.0769	0.0011	0.6550	0.0131	0.0605	0.0005	478	7	616	19	22
12.1	0.0985	0.0009	0.8148	0.0109	0.0602	0.0005	606	5	605	18	0
13.1	0.0939	0.0009	0.7842	0.0117	0.0604	0.0005	578	5	611	19	5
14.1	0.1007	0.0008	0.8357	0.0114	0.0606	0.0003	618	5	619	12	0
15.1	0.0986	0.0009	0.8278	0.0113	0.0610	0.0004	606	5	633	13	4
16.1	0.0956	0.0008	0.7959	0.0111	0.0601	0.0004	588	5	602	14	2
17.1	0.1073	0.0010	0.9109	0.0129	0.0617	0.0004	657	6	657	13	0
18.1	0.1038	0.0008	0.8740	0.0116	0.0607	0.0003	637	5	622	11	-2
19.1	0.1084	0.0012	0.9243	0.0144	0.0618	0.0004	663	7	661	15	0
20.1	0.1024	0.0008	0.8638	0.0114	0.0609	0.0003	628	5	629	12	0
21.1	0.1021	0.0008	0.8550	0.0109	0.0609	0.0003	627	5	629	11	0
22.1	0.0898	0.0008	0.7284	0.0102	0.0604	0.0004	554	5	612	13	9
23.1	0.0716	0.0012	0.5682	0.0126	0.0572	0.0004	446	7	495	17	10
24.1	0.1016	0.0008	0.8531	0.0111	0.0610	0.0003	624	5	632	12	1
25.1	0.0923	0.0008	0.7663	0.0106	0.0599	0.0004	569	5	594	14	4
26.1	0.1060	0.0009	0.8941	0.0118	0.0612	0.0003	649	5	640	11	-1
27.1	0.1046	0.0005	0.8714	0.0096	0.0607	0.0006	641	3	621	21	-3
28.1	0.0903	0.0009	0.7405	0.0120	0.0598	0.0006	557	6	589	22	5
29.1	0.0991	0.0005	0.8363	0.0095	0.0611	0.0006	609	3	636	21	4
30.1	0.1036	0.0006	0.8701	0.0104	0.0611	0.0006	635	4	638	20	0
31.1	0.0892	0.0005	0.7397	0.0095	0.0599	0.0006	551	3	592	23	7
32.1	0.1025	0.0005	0.8608	0.0096	0.0609	0.0006	629	3	629	20	0
33.1	0.0955	0.0005	0.8052	0.0091	0.0609	0.0006	588	3	628	21	6
34.1	0.1074	0.0007	0.8942	0.0106	0.0611	0.0006	658	4	636	21	-3
35.1	0.1026	0.0005	0.8647	0.0094	0.0615	0.0006	630	3	649	20	3
36.1	0.0940	0.0006	0.7908	0.0095	0.0600	0.0006	579	3	597	21	3
37.1	0.1005	0.0005	0.8343	0.0100	0.0605	0.0006	617	3	617	21	0
38.1	0.1051	0.0005	0.8905	0.0095	0.0611	0.0006	644	3	635	20	-1
39.1	0.1030	0.0006	0.8737	0.0103	0.0616	0.0006	632	4	653	20	3
40.1	0.0909	0.0009	0.7356	0.0123	0.0589	0.0009	561	6	559	33	0
41.1	0.1053	0.0008	0.8883	0.0104	0.0613	0.0007	645	5	643	26	0
42.1	0.0923	0.0007	0.7958	0.0094	0.0626	0.0007	569	4	689	26	17
43.1	0.1042	0.0009	0.9118	0.0123	0.0630	0.0008	639	5	704	27	9
44.1	0.1020	0.0010	0.8564	0.0112	0.0608	0.0008	626	6	627	27	0
45.1	0.0934	0.0010	0.7626	0.0120	0.0594	0.0008	575	6	576	28	0
46.1	0.1047	0.0010	0.8847	0.0113	0.0613	0.0007	642	6	643	26	0
47.1	0.0852	0.0013	0.6330	0.0153	0.0599	0.0017	527	8	595	61	11
48.1	0.0905	0.0009	0.7561	0.0113	0.0605	0.0008	559	5	615	29	9
49.1	0.1003	0.0009	0.8316	0.0115	0.0606	0.0009	616	5	618	30	0
50.1	0.1054	0.0009	0.8869	0.0109	0.0614	0.0007	646	5	646	26	0
51.1	0.0996	0.0008	0.8366	0.0100	0.0612	0.0007	612	5	640	26	4
52.1	0.2266	0.0025	4.6865	0.0707	0.1524	0.0018	1317	13	2368	21	44
53.1	0.0941	0.0003	0.7836	0.0057	0.0606	0.0004	580	2	619	13	6
54.1	0.1018	0.0002	0.8635	0.0044	0.0614	0.0003	625	1	647	10	3
55.1	0.0984	0.0006	0.8269	0.0072	0.0610	0.0003	605	4	632	12	4
56.1	0.0969	0.0003	0.8197	0.0048	0.0615	0.0003	596	2	651	10	8
57.1	0.0974	0.0002	0.8139	0.0048	0.0612	0.0004	599	1	639	12	6
58.1	0.1002	0.0003	0.8402	0.0052	0.0605	0.0003	616	1	616	12	0
59.1	0.0996	0.0003	0.8388	0.0046	0.0612	0.0003	612	2	640	11	4
60.1	0.1053	0.0004	0.8886	0.0091	0.0613	0.0006	645	3	646	19	0
61.1	0.0926	0.0003	0.7584	0.0048	0.0596	0.0004	571	2	582	13	2

(continued on next page)

**Table 5** (continued)

Grão. spot	Radiogenic ratios						Age (Ma)			% disc	
	$^{206}\text{Pb}/^{238}\text{U}$	±	$^{207}\text{Pb}/^{235}\text{U}$	±	$^{207}\text{Pb}/^{206}\text{Pb}$	±	$^{206}\text{Pb}/^{238}\text{U}$	±	$^{207}\text{Pb}/^{206}\text{Pb}$		
62.1	0.0816	0.0008	0.6166	0.0102	0.0575	0.0006	506	4	504	22	0
63.1	0.0984	0.0005	0.8153	0.0063	0.0606	0.0003	605	3	620	12	2
64.1	0.1035	0.0003	0.8704	0.0047	0.0610	0.0003	635	2	633	11	0
65.1	0.0977	0.0003	0.8125	0.0051	0.0603	0.0004	601	2	610	14	1

Note: Errors are 1-sigma.

$^{86}\text{Sr}$  ratios ( $\sim 0.7075$ ) reported for both sequences is another evidence that this gap is much shorter or does not exist, as already discussed by Caxito et al. (2012). Therefore, the youngest voluminous zircon population ( $\sim 557$  Ma) sets the maximum depositional age for the Sete Lagoas Formation and most of the Bambuú Group. This age is consistent with the recently found index fossil *Cloudina* in this unit (Warren et al., 2014), which is thought to have lived between 550 and 543 Ma (Grotzinger et al., 2000).

If there is a major gap of sedimentation within the Sete Lagoas Formation, it is positioned between the basal cap carbonate sequence and the succeeding carbonates that preserve higher  $\delta^{13}\text{C}$  values of around 0‰. No erosive unconformity surface is known from here. In this work, no geochronological data were obtained from the basal cap carbonates with  $\delta^{13}\text{C}$  values as low as  $-4.5\text{\textperthousand}$ , which would be equivalent of the one previously dated at  $740 \pm 22$  Ma (Babinski et al., 2007).

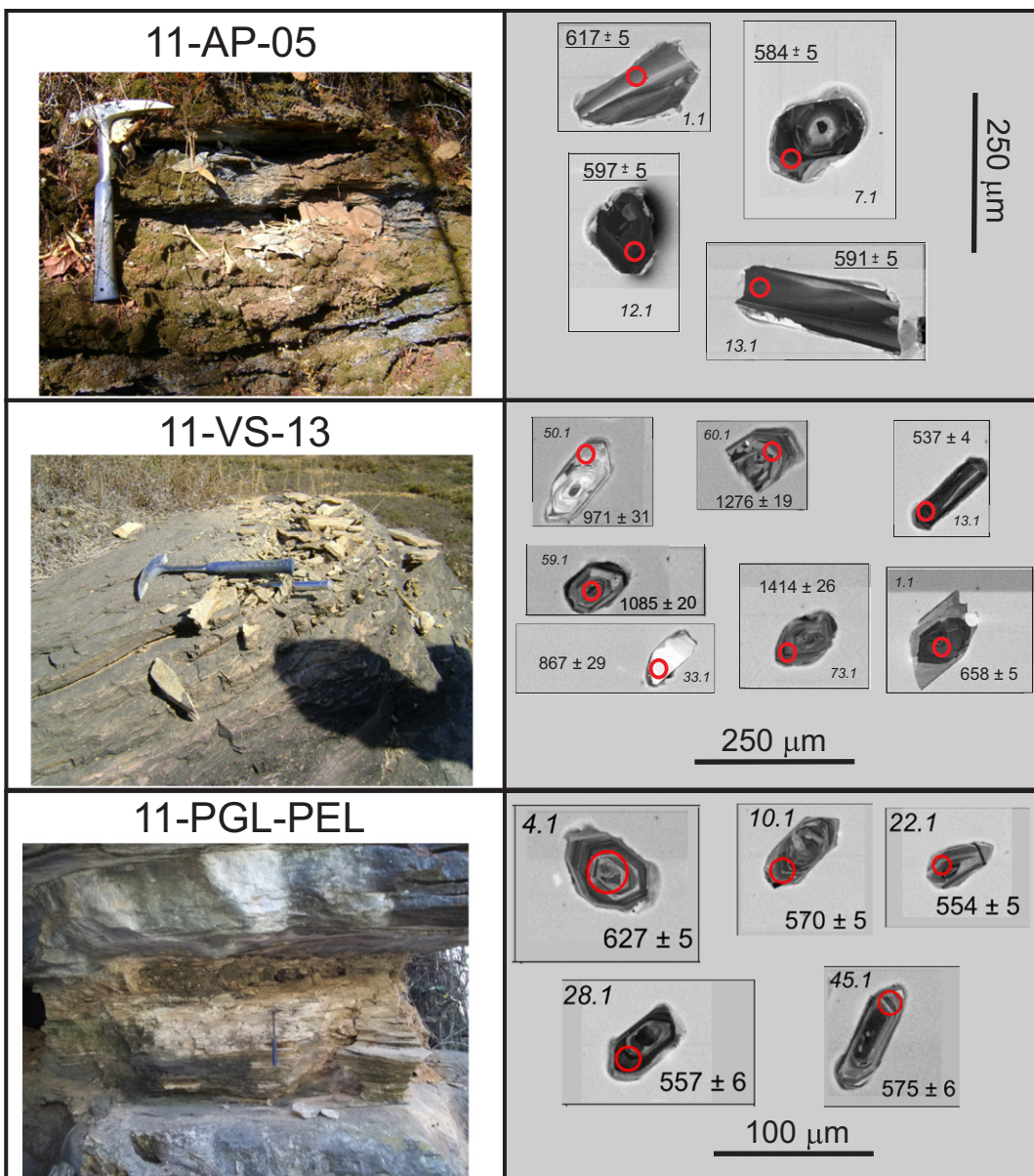


**Fig. 4.** Field images of the marl samples (hammer is  $\sim 30$  cm tall) and their respective cathodoluminescence images of the retrieved zircon grains.

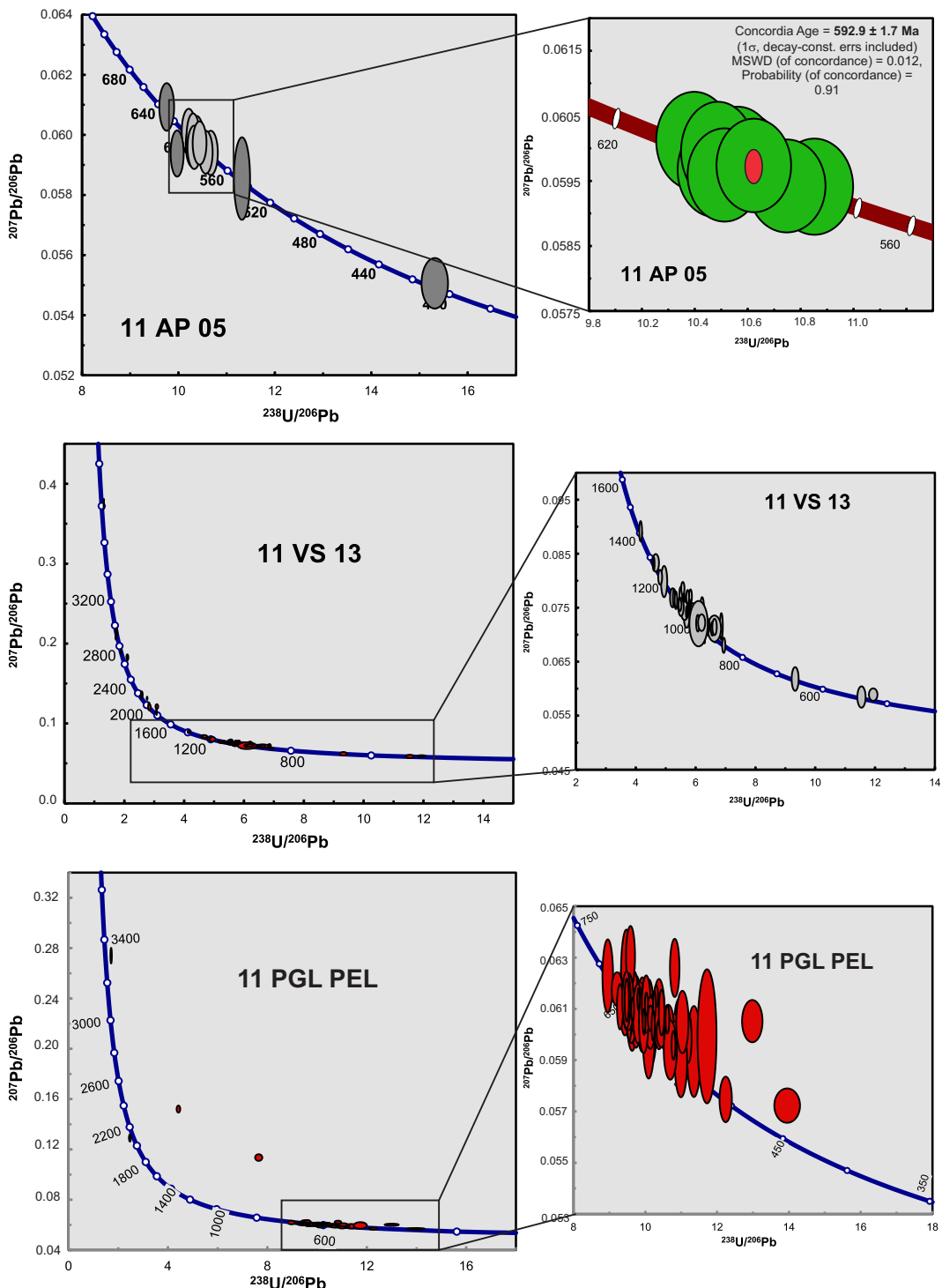


**Fig. 5.** Tera and Wasserburg (1972) concordia diagram obtained for the marl samples.

Other important implications of the obtained ages concern the tectonic framework of the São Francisco Craton during the deposition of the Bambuí Group. The maximum depositional age around 560 Ma suggests that most of the Sete Lagoas Formation was deposited after the closure of the Adamastor Ocean. At that time, the Araçuaí–West Congo orogen already existed to the east of the São Francisco Craton. This suggests that the marine units of the Bambuí Group were probably deposited in a restricted sea, confined by the marginal belts surrounding the São Francisco Craton in the late Ediacaran. This scenario is consistent with our geochronological data that points to the post-collisional supersuites of the Araçuaí Belt acting as sources to the Sete Lagoas

Formation. In addition, if the sources of the 1400–900 Ma zircon grains in the Sete Lagoas Formation are from the Macaúbas Group sediments, this unit was already partially exhumed within the margin of the orogen. Interestingly, the basal sample (11-VS-13) shows a wide distribution of detrital zircon ages (Fig. 6) whose rounded morphology suggests some degree of sedimentary reworking (Fig. 4). The distribution of ages for this sample resembles those obtained for the glacial deposits of Macaúbas Group (Babinski et al., 2012). In contrast, the sample collected in the upper unit provides only Ediacaran peaks of zircon ages (Fig. 6), which match the different generations of granites mapped in the Araçuaí Belt (Pedrosa-Soares et al., 2011a, 2011b). This source

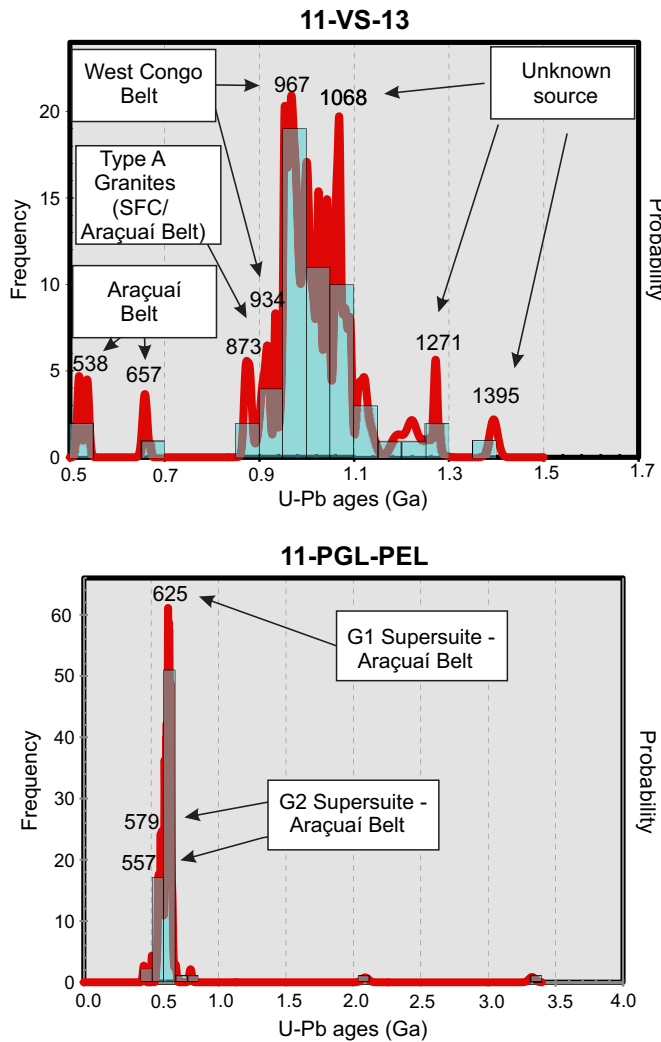


**Fig. 6.** Histogram obtained with U-Pb ages from detrital zircons retrieved from samples 11-VS-13 and 11-PGL-PEL. Only ages within the 90–110% concordance interval were considered.

change suggests that the filling of the Bambuí basin is, at least partially, coeval with uplifting of the Araçuaí Belt.

The restricted basin scenario proposed here requires additional study. However, some evidence seems to support a confined epeiric sea. The presence of *Cloudina* in the Sete Lagoas Formation suggests ocean connectivity among coeval intracratonic basins of South America, Africa and Antarctica at the Ediacaran–Cambrian boundary (Warren et al., 2014). However, unlike the other Ediacaran units, the Sete Lagoas Formation yields  $^{87}\text{Sr}/^{86}\text{Sr}$  ratios lower than those expected when compared to Neoproterozoic seawater Sr evolution curves. While it displays ratios around 0.7075, the curves presuppose ratios higher than 0.7080 (Jacobsen and Kaufman, 1999; Melezhik et al., 2001; Halverson et al., 2010; Kusnetsov et al., 2013). Other South American carbonate *Cloudina*-bearing successions such as the Corumbá and the Arroyo del Soldado groups display  $^{87}\text{Sr}/^{86}\text{Sr}$  ratios higher than 0.7080 (Boggiani, 1998; Gaucher et al., 2004; Boggiani et al., 2010). This probably means that these two units were thoroughly linked to the global ocean, whereas the Bambuí Group was not. This also suggests that the connections of the São Francisco Craton epeiric sea with other intracratonic Ediacaran marine basins were possibly intermittent and short lived. This prevented constant and significant mixing of the São Francisco Craton seawaters with others coming from external basins, resulting in different Sr isotope ratios. In fact, the *Cloudina* specimens described in the Sete Lagoas Formation were found on carbonates with  $\delta^{13}\text{C}$  of around 0‰ and from

the top of the basal sequence (Warren et al., 2014). So the occurrence of the fossil precedes the abrupt shift on C isotope values close to the sequence boundary. It is possible that this marked positive excursion of the C isotope values sets the changing of an intracontinental basin sporadically linked to other basins by an proto-Gondwana seaway to an restricted basin with  $\delta^{13}\text{C}$  values much higher than those of the Corumbá and the Arroyo del Soldado groups (Gaucher et al., 2004; Boggiani et al., 2010) that could not be explained only by bioproductivity increase or organic matter burial. The hypothesis of fermentation-related methanogenesis and direct reduction of  $\text{CO}_2$  in a restricted environment has to be considered to explain  $\delta^{13}\text{C}$  values as high as +14‰. The Sr content of the upper sequence carbonates (as high as 3500 ppm) are also flagrantly higher than those described for Ediacaran units as well as than those considered for the Sr seawater evolution curve calibration (Jacobsen and Kaufman, 1999; Melezhik et al., 2001; Halverson et al., 2010; Kusnetsov et al., 2013). This could be a result of enhanced evaporation due to the basin confinement, a process that could also lead to higher  $\delta^{13}\text{C}$  values (Frimmel, 2010). It is worth mentioning that the debate of the meaning of the chemostratigraphy data of the Bambuí Group is still speculative and needs more detailed studies.

Other problems concerning an Ediacaran age for the Sete Lagoas Formation regard the tectonic relationship between the deposition of the Bambuí Group and the geological evolution of the São Francisco Craton marginal belts. A large dataset, including field relations, distribution and nature of sedimentary rocks, seismic and gravimetric data, suggests that the Bambuí Group was deposited in a foreland basin, with flexural subsidence mainly induced by crustal loading by the Brasília Belt (Martins-Neto et al., 2001; Coelho et al., 2008). The timing of mountain building and sediment accumulation along the foreland is constrained by data from the magmatic units within the belt and detrital zircons in the sediments. Collisional ages in the Brasília Belt obtained mostly from its prominent granitic magmatism suggest that the peak of collision has occurred at ~620 Ma (e.g., Pimentel et al., 1999; Pimentel et al., 2011). Recent provenance studies based on zircon dating in sedimentary units at the western border of the São Francisco Craton show ages older than 930 Ma for the Vazante Group, similar to the pattern observed for the diamictites (Rodrigues et al., 2012). Thus, sedimentary successions deposited at the base of the Bambuí Group seem to pre-date the orogeny buildup. Abundant Neoproterozoic ages, which would ascertain a Brasília Belt provenance, are found only in the Três Marias Formation, the uppermost unit of the Bambuí Group (Pimentel et al., 2001; Pimentel et al., 2011). Our new data provide better temporal constraints to these events, since it places a maximum depositional age for the base of the Bambuí Group at around 560 Ma, suggesting that foreland sedimentation in the craton has started later than previously thought. In fact, our data shows that the Sete Lagoas Formation sedimentation is coeval with the construction of the Araçuaí Belt and may have been strongly influenced by it (Pedrosa-Soares et al., 2011a, 2011b). Nevertheless, the time span between the supposed flexural subsidence (~620 Ma; Pimentel et al., 1999; Pimentel et al., 2011) and the start of the sedimentation (~560 Ma) is too long and problematic. Other subsidence mechanisms might have occurred or some geochronological piece of the puzzle is missing. This also is valid to explain why the Bambuí Group is deformed on its western border as the Brasília orogen would be in its collapse phase during the late Ediacaran (Pimentel et al., 1999).

### 5.3. U-Pb dating vs. Sr “blind dating”: some considerations

The U-Pb data of detrital zircons and Sr isotope data from carbonates clearly provides different age constrains for the Sete Lagoas Formation. The commonly reported  $^{87}\text{Sr}/^{86}\text{Sr}$  ratios around 0.7075 for the unit (Alvarenga et al., 2007; Misi et al., 2007; Kuchenbecker, 2011; this work) are significantly less radiogenic than those expected for the end of Ediacaran according to several Sr isotope composition evolution curves and compilations (Jacobsen and Kaufman, 1999; Melezhik et al.,

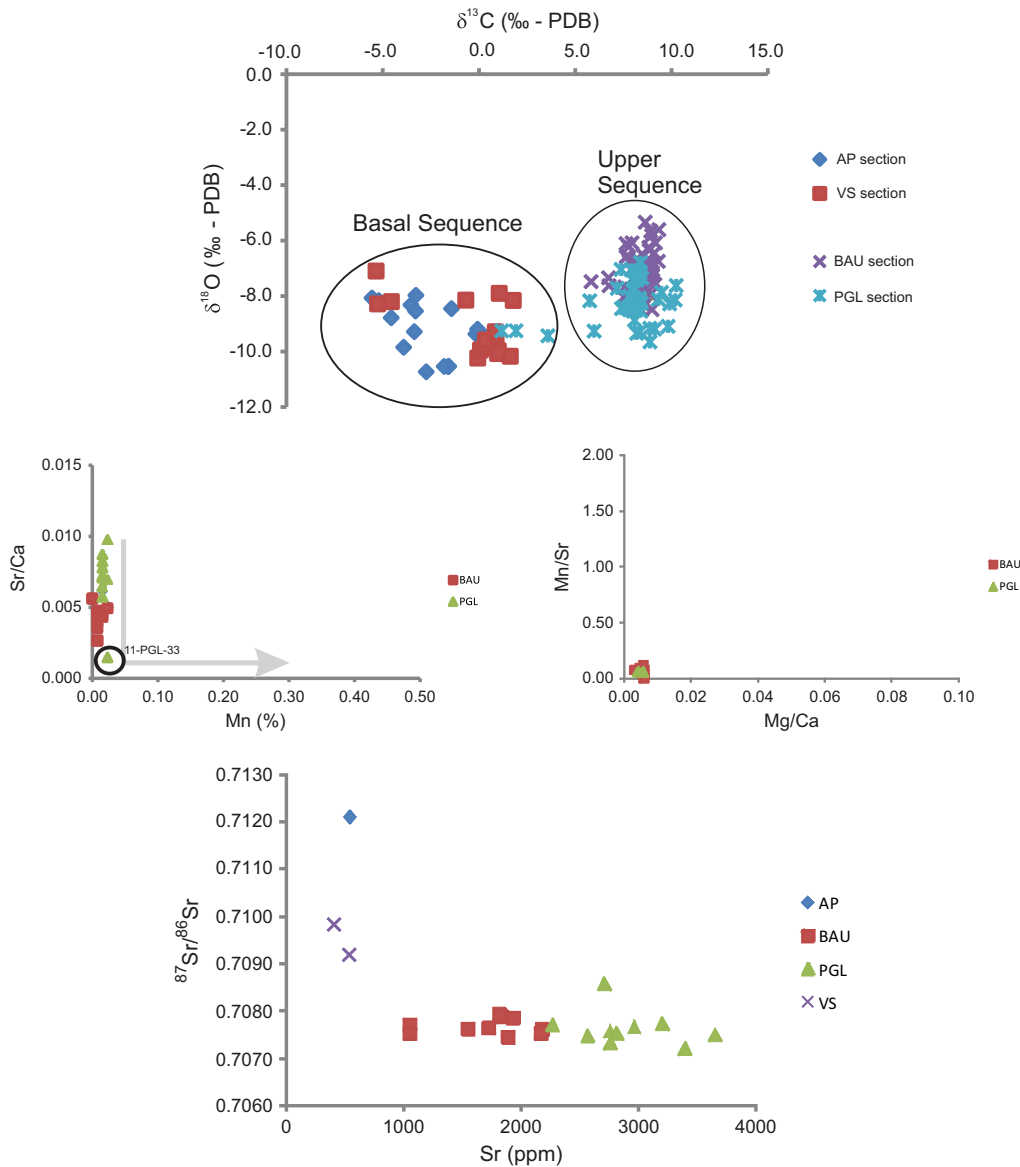


**Fig. 7.**  $\delta^{13}\text{C}$  vs.  $\delta^{18}\text{O}$ , Mn (%) vs. Sr/Ca, Mg/Ca vs. Mn/Sr and Sr (ppm) vs.  $^{87}\text{Sr}/^{86}\text{Sr}$  geochemical diagrams of the carbonates of SLF.

2001; Halverson et al., 2010; Kusnetsov et al., 2013).  $^{87}\text{Sr}/^{86}\text{Sr}$  ratios higher than 0.7080 were expected for a carbonate succession younger than 560 Ma. Additionally, other *Cloudina*-bearing carbonate successions in South America also display ratios higher than 0.7080 (Boggiani, 1998; Gaucher et al., 2004; Boggiani et al., 2010).

As previously discussed, the tectonic framework of the São Francisco Craton during the Ediacaran could explain such discrepancy. During that period, the craton was almost completely surrounded by fold belts and was located at the inner parts of the western Gondwana continent (Pedrosa-Soares et al., 2011a, 2011b; Alkmin and Martins-Neto, 2012). Such a scenario strongly suggests a restricted marine basin. The presence of the index fossil *Cloudina* suggests connection with other Ediacaran marine basins, but the non-radiogenic Sr ratios show that such connection was possibly intermittent and short lived, preventing efficient mixing of the São Francisco Craton seawaters with others coming from external basins.

One possibility to explain the Sr isotopic discrepancy is that this restricted sea could possibly have received large amounts of riverine freshwater and little external seawater, implying in a different isotope evolution from contemporaneous global ocean. It is known that the riverine influx is the main factor controlling the Sr budget on modern

oceans (Goldstein and Jacobsen, 1987; Palmer and Edmond, 1989), and there is no reason to believe otherwise for restricted environments. However, most of modern rivers have  $^{87}\text{Sr}/^{86}\text{Sr}$  ratios higher than the modern oceans (Goldstein and Jacobsen, 1987; Palmer and Edmond, 1992; Gaillardet et al., 1997), and thus is expected that a restricted basin should display higher ratios than the contemporaneous global ocean. But there are some exceptions. The São Francisco Craton epeiric sea is most likely to have received riverine freshwater draining the uplifted areas with typical lithology assembly from mobile belts (quartzites, pelites and carbonates, granites and trapped basement rocks). Modern rivers draining similar areas are usually Sr enriched and have lower  $^{87}\text{Sr}/^{86}\text{Sr}$  ratios than contemporaneous global ocean due to preferential carbonate leaching on highland areas (Palmer and Edmond, 1992). If a similar process occurred in the São Francisco Craton, the continuously delivering of freshwaters rich in Sr and with low  $^{87}\text{Sr}/^{86}\text{Sr}$  ratios may have progressively lowered the ratio of the restricted sea. Although our geochronological data suggest that the Araçuaí Orogen, with no significant older carbonate successions, is the main source of the Bambuí Group in the southeast of the São Francisco Craton, at a regional scale the basin might have received waters from rivers draining areas where ancient carbonates were exposed. Examples of

carbonate successions older than the Sete Lagoas Formation and with lower  $^{87}\text{Sr}/^{86}\text{Sr}$  ratios are the Paranoá Group (Alvarenga et al., 2007) and the Vazante Group (Azmy et al., 2001) in western Brasília Belt. To evaluate if carbonate weathering contribution to the Sr ratios of the Bambuí Group was more important than silicate weathering, additional studies using other proxies are necessary, as the current database is insufficient.

Although our claimed scenario seems possible, recently published studies have shown that the Sr isotope composition of modern marginal and inland seas barely differ from the global ocean (Kusnetsov et al., 2012). The case of the Black Sea is the most intriguing, because its seawater dilution by riverine runoff is as high as 50 to 70%, and could be somewhat similar to the Bambuí basin. However, two statements must be addressed: (i) the Black Sea is often filled with external marine water (Kusnetsov et al., 2012) and data from the fossil record and Sr isotopes suggest short lived and inefficient external water mixing in the São Francisco Craton; and (ii) values of riverine  $^{87}\text{Sr}/^{86}\text{Sr}$  ratios delivered to the Black Sea are unknown. Curiously, the only value measured (not inferred) is 0.7127 (Krabbenhoft et al., 2010) which is higher than the world's riverine average delivered to oceans. This would imply in a Sr composition evolution of the Black Sea similar to that of the global ocean.

The cause of the lower  $^{87}\text{Sr}/^{86}\text{Sr}$  ratios of the Sete Lagoas Formation notwithstanding, the fact is that they clearly disagree with our U-Pb data on detrital zircons and the fossil assemblage of the unit. Other examples of such discrepancy are the Lantian Formation and Doushantuo Formation in South China. The Ediacaran upper unit of the Lantian Formation has  $^{87}\text{Sr}/^{86}\text{Sr}$  ratios higher than 0.71 that strongly differs from the contemporaneous global ocean (Zhao et al., 2009). Anomalously high  $^{87}\text{Sr}/^{86}\text{Sr}$  ratios (~0.71) are also reported for the Doushantuo Formation (Ohno et al., 2008), deposited between 635 and 551 Ma (Condon et al., 2005). In both cases, the large disturbance in Sr composition of the ancient seawaters was attributed to local processes rather than to a global one. Frimmel (2009) proposed that these local variations were common in the Ediacaran when near-shore basins were flooded with continental freshwater with little exchange with global seawaters. The restriction of the marine basin in which the Bambuí Group was deposited contradicts an important premise for worldwide correlations using isotope chemostratigraphy (Melezhik et al., 2001). The C and Sr composition of the carbonates of the Sete Lagoas Formation probably reflects the composition of the former restricted seawaters rather than the composition of the global contemporaneous ocean. We therefore recommend caution on correlating the Sete Lagoas Formation and the Bambuí Group to other carbonate successions worldwide by using isotope chemostratigraphy. It is also recommended to use extreme caution on strontium "blind dating", especially in Ediacaran carbonate successions. U-Pb dating on detrital zircon grains is a more reliable tool for age constraining and tracing the tectonic setting (Cawood et al., 2012). If dating of detrital minerals is not possible, the Sr blind dating should be performed very carefully, analysing the tectonic framework in which the carbonate succession was deposited and checking different Sr evolution curves for age constraining.

## 6. Conclusions

The C and Sr isotope and the U-Pb geochronological data obtained in this work provided a new insight on the depositional age and sedimentary evolution of the Sete Lagoas Formation. Such data were obtained on sections from the upper sequence of the unit composed of dark carbonates with highly positive  $\delta^{13}\text{C}$  values ( $> +6\text{\textperthousand}$ ) and from the basal sequence composed of carbonates with  $\delta^{13}\text{C}$  values around 0‰, stratigraphically above the basal cap carbonates.

Marl samples from AP and PGL sections (basal and upper sequence respectively) provided detrital zircon grains with U-Pb ages mainly ranging between 625 and 550 Ma. These data strongly suggest that the Araçuaí orogen, located east of the São Francisco Craton, was a

sedimentary source acting during the deposition of the Sete Lagoas Formation in the studied area. Sample 11-VS-13 displayed several zircon populations with dominant ages between 1270 and 870 Ma that also suggest the Araçuaí–West Congo Orogen as the main source. The similarity of these populations to those found on the Macaúbas Group (Araçuaí Belt) suggests that the sediments found within VS section could be redeposited from that group.

The youngest voluminous zircon population of ~557 Ma sets the maximum depositional age for most of the Sete Lagoas Formation and the Bambuí Group at around 560 Ma, which is supported by the recently found Ediacaran fauna. A concordia maximum depositional age of  $593 \pm 1.7$  Ma was obtained for the basal sequence and no significant hiatus is expected across the sequence boundary. These data do not support the possibility of a major gap of about 130 Ma within the sedimentation of this unit after the basin drowning that ended the basal sequence. If there is such gap, it is positioned between the lowermost cap carbonates dated in  $740 \pm 22$  Ma (Babinski et al., 2007) with very negative  $\delta^{13}\text{C}$  values and the carbonates with  $\delta^{13}\text{C}$  values around 0‰.

Our U-Pb ages on detrital zircons suggest that the sedimentation of most of the Bambuí Group (at least in the eastern portion of the basin) started at the late Ediacaran and occurred on a restricted type basin, after the closure of the Adamastor Ocean and the build-up of the Araçuaí–West Congo Orogen to the east of the São Francisco Craton. The marine units were probably deposited on a restricted sea that did not homogenize its isotopic composition with the contemporaneous global ocean. This hypothesis is supported by the discrepancy between the  $^{87}\text{Sr}/^{86}\text{Sr}$  ratios obtained for the Sete Lagoas Formation carbonates (~0.7075) and those expected for the late Ediacaran (>0.7080). Such discrepancy is also reported for other Ediacaran units worldwide. Therefore, extreme caution is required for global correlations and Sr "blind dating" of Ediacaran–Cambrian carbonate successions deposited on epicontinental seas.

## Acknowledgements

The authors would like to thank the staff of the Geochronological Research Center of University of São Paulo for all the support given on the data acquirement. We also thank the Geotectonics and Regional Mapping Laboratory of the Federal University of Minas Gerais for the logistics and field work support, and two anonymous reviewers that greatly contributed to improve this work. This project was financed by FAPESP (05/58688).

## References

- Alkmim, F.F., Marshak, S., Pedrosa-Soares, A.C., Peres, G.G., Cruz, S.C., Whittington, A., 2006. Kinematic evolution of the Araçuaí–West Congo orogen in Brazil and Africa: nutcracker tectonics during the Neoproterozoic assembly of Gondwana. *Precambrian Research* 149, 43–63.
- Alkmim, F.F., Martins-Neto, M.A., 2012. Proterozoic first-order sedimentary sequences of the São Francisco craton, eastern Brazil. *Marine and Petroleum Geology* 33 (1), 127–139.
- Alvarenga, C.J.S., Santos, R.V., Dantas, E.L., 2004. C–O–Sr isotopic stratigraphy of cap carbonates overlying Marinoan-age glacial diamictites in the Paraguay Belt, Brazil. *Precambrian Research* 131, 1–21.
- Alvarenga, C.J.S., Della Giustina, M.E.S., Silva, N.G.C., Santos, R.V.S., Gioia, S.M.C.L., Guimarães, E.M., Dardenne, M.A., Sial, A.N., Ferreira, V.P., 2007. Variações dos isótopos de C e Sr em carbonatos pré e pós-glaciação Jequitáí (Esturtiano) na região de Bezerra-Formosa, Goiás. *Revista Brasileira de Geociências* 37 (4), 147–155.
- Alvarenga, C.J.S., Dardenne, M.A., Santos, R.V., Brod, E.R., Gioia, S.M.C.L., Sial, A.N., Dantas, E.L., Ferreira, V.P., 2008. Isotope stratigraphy of Neoproterozoic cap carbonates in the Araras Group, Brazil. *Gondwana Research* 13, 469–479.
- Azmy, K., Veizer, J., Misi, A., Oliveira, T.F., Sanches, A.L., Dardenne, M.A., 2001. Dolomitization and isotope stratigraphy of the Vazante Formation, São Francisco Basin, Brazil. *Precambrian Research* 112 (3–4), 303–329.
- Babinski, M., Vieira, L.C., Trindade, R.I.F., 2007. Direct dating of Sete Lagoas cap carbonate (Bambuí Group, Brazil) and implications for the Neoproterozoic glacial events. *Terra Nova* 19, 401–406.
- Babinski, M., Pedrosa-Soares, A.C., Trindade, R.I.F., Martins, M., Noce, C.M., Liu, D., 2012. Neoproterozoic glacial deposits from the Araçuaí orogen, Brazil: age, provenance

- and correlations with the São Francisco craton and West Congo belt. *Gondwana Research* 21, 451–465.
- Boggiani, P.C., 1998. Análise estratigráfica da Bacia Corumbá (Neoproterozoico) – Mato Grosso do Sul. (PhD thesis) Universidade de São Paulo, Instituto de Geociências, (181 pp.).
- Boggiani, P.C., Gaucher, C., Sial, A.N., Babinski, M., Simon, C.M., Riccomini, C., Ferreira, V.P., Fairchild, T.R., 2010. Chemostratigraphy of the Tamengo Formation (Corumbá Group, Brazil): a contribution to the calibration of the Ediacaran carbon-isotope curve. *Precambrian Research* 182 (4), 382–401.
- Brand, U., Veizer, J., 1980. Chemical diagenesis of a multicomponent carbonate system-1: trace elements. *Journal of Sedimentary Petrology* 50, 1219–1236.
- Brito-Neves, B.B., Campos-Neto, M.C., Fuck, R.A., 1999. From Rodinia to Western Gondwana: an approach to the Brasiliano – Pan African Cycle and orogenic collage. *Episodes* 22, 155–166.
- Buchwaldt, R., Toulkeridis, T., Babinski, M., Santos, R., Noce, C.M., Martins-Neto, M.A., Hercos, C.M., 1999. Age determination and age-related provenance analysis of the Proterozoic glaciation event in central-eastern Brazil. *South American Symposium on Isotope Geology*, 2, Cordoba, Argentina, *Actas*, pp. 387–390.
- Cawood, P.A., Hawkesworth, C.J., Dhuime, B., 2012. Detrital zircon and tectonic record. *Geology* 40, 875–878.
- Caxito, F.A., Halverson, G.P., Uhlein, A., Stevenson, R., Dias, T.G., Uhlein, G.J., 2012. Marinoan glaciation in east Central Brazil. *Precambrian Research* 200–203, 38–58.
- Chemale, F., Dussin, I.A., Alkmim, F.F., Martins, M.S., Queiroga, G., Armstrong, R., Santos, M.N., 2012. Unravelling a Proterozoic basin history through detrital zircon geochronology: the case of the Espinhaço Supergroup, Minas Gerais, Brazil. *Gondwana Research* 22 (1), 200–206.
- Coelho, J.C.C., Martins-Neto, M.A., Marinho, M.S., 2008. Estilos estruturais e evolução tectônica da porção mineira da bacia proterozóica do São Francisco. *Revista Brasileira de Geociências* 38 (2), 149–165.
- Condon, D., Zhu, M., Bowring, S., Wang, W., Yang, A., Jin, Y., 2005. U-Pb ages from the Neoproterozoic Doushantu Formation, China. *Science* 308, 95–98.
- Cordani, U.G., Brito-Neves, B.B., D'agrella-Filho, M.S., Trindade, R.I.F., 2003. Tearing-up Rodinia: the Neoproterozoic paleogeography of South American cratonic fragments. *Terra Nova* 15, 343–349.
- Dardenne, M.A., 1978. Síntese sobre a estratigrafia do Grupo Bambuí no Brasil Central. SBG, Congresso Brasileiro de Geologia, 30, Recife, Brazil. Anais. v. 2, pp. 597–610.
- Dardenne, M.A., 2000. The Brasília fold belt. In: Cordani, U.G., Milani, E.J., Thomaz-Filho, A., Campos, D.A. (Eds.), *Tectonic Evolution of South America*. 31st International Geological Congress, Rio de Janeiro, pp. 231–263.
- Derry, L.A., 2010. A burial diagenesis origin for the Ediacaran Shuram–Wonka carbon isotope anomaly. *Earth and Planetary Science Letters* 294, 152–162.
- Derry, L.A., Kaufman, A.J., Jacobsen, S.B., 1992. Sedimentary cycling and environmental change in the Late Proterozoic: evidence from stable and radiogenic isotopes. *Geochimica et Cosmochimica Acta* 56, 1317–1329.
- Ehlou, S., Belousova, E., Griffin, W.L., Pearson, N.J., O'Reilly, S.Y., 2006. Trace element and isotopic composition of GJ-red zircon standard by laser ablation. *Geochimica et Cosmochimica Acta* 70 (18), A158.
- Fölling, P.G., Frimmel, H.E., 2002. Chemostratigraphic correlation of carbonate successions in the Gariep and Saldanha Belts, Namibia and South Africa. *Basin Research* 14, 69–88.
- Frimmel, H.E., 2009. Trace element distribution in Neoproterozoic carbonates as palaeoenvironmental indicator. *Chemical Geology* 258, 338–353.
- Frimmel, H.E., 2010. On the reliability of stable carbon isotopes for Neoproterozoic chemostratigraphic correlation. *Precambrian Research* 182 (4), 239–253.
- Gaillardet, J., Dupré, B., Allegre, C.J., Négrelle, P., 1997. Chemical and physical denudation in the Amazon River Basin. *Chemical Geology* 142 (3–4), 141–173.
- Gaucher, C., Sial, A.N., Blanco, G., Sprechmann, P., 2004. Chemostratigraphy of the Lower Arroyo del Soldado Group (Vendian, Uruguay) and paleoclimatic implications. *Gondwana Research* 7 (3), 715–730.
- Goldstein, S.J., Jacobsen, S.B., 1987. The Nd and Sr isotopic systematic of river-water dissolved material: implications for the sources of Nd and Sr in seawater. *Chemical Geology: Isotope Geoscience Section* 66 (3–4), 245–272.
- Grotzinger, J.P., Knoll, A.H., 1995. Anomalous carbonate precipitates: is the Precambrian the key to the Permian? *Palaios* 10, 578–596.
- Grotzinger, J.P., Waters, W.A., Knoll, A.H., 2000. Calcified metazoans in thrombolite-stromatolite reefs of the terminal Proterozoic Nama Group, Namibia. *Paleobiology* 26 (3), 334–359.
- Halverson, G.P., Dudás, F.O., Maloof, A.C., Bowring, S.A., 2007. Evolution of the  $^{87}\text{Sr}/^{86}\text{Sr}$  composition of Neoproterozoic seawater. *Palaeogeography, Palaeoclimatology, Palaeoecology* 256 (3–4), 103–129.
- Halverson, G.P., Wade, B.P., Hurtgen, M.T., Barovich, K.M., 2010. Neoproterozoic chemostratigraphy. *Precambrian Research* 182, 337–350.
- Heilbron, M., Tupinambá, M., Valeriano, C.M., Armstrong, R., Siva, L.G.E., Melo, R.S., Simonetti, A., Pedrosa-Soares, A.C., Machado, N., 2013. The Serra Bolívia Complex: the record of a new Neoproterozoic arc-related unit at Ribeira Belt. *Precambrian Research* 238, 158–175.
- Hoffman, P.F., Schrag, D.P., 2002. The Snowball Earth hypothesis: testing the limits of global change. *Terra Nova* 14, 129–155.
- Iyer, S.S., Babinski, M., Krouse, H.L., Chemale, F., 1995. Highly  $^{13}\text{C}$  enriched carbonate and organic matter in the Neoproterozoic sediments of the Bambuí Group, Brazil. *Precambrian Research* 73, 271–282.
- Jacobsen, S.B., Kaufman, A.J., 1999. The Sr, C and O isotopic evolution of Neoproterozoic seawater. *Chemical Geology* 161, 37–57.
- Jones, C.E., Jenkyns, 2001. Seawater strontium isotopes, oceanic anoxic events, and seafloor hydrothermal activity in the Jurassic and Cretaceous. *American Journal of Science* 301, 112–149.
- Karfunkel, J., Hoppe, A., 1988. Late Precambrian glaciation in central-eastern Brazil: synthesis and model. *Palaeogeography Palaeoclimatology Palaeoecology* 65, 1–21.
- Kennedy, M.J., 1996. Stratigraphy, sedimentology, and isotope geochemistry of Australian Neoproterozoic postglacial cap dolostones: deglaciation,  $\delta^{13}\text{C}$  excursions, and carbonate precipitation. *Journal of Sedimentology Research* 66, 1050–1064.
- Krabbenhöft, A., Eisenhauer, A., Böhm, F., Vollstaedt, H., Fietzke, J., Liebetrau, V., Augustin, N., Peucker-Ehrenbrink, B., Müller, M.N., Horn, C., Hansen, B.T., Nolte, N., Wallmann, K., 2010. Constraining the marine strontium budget with natural strontium isotope fractionations ( $^{87}\text{Sr}/^{86}\text{Sr}^*$ ,  $d^{88}\text{Sr}/^{86}\text{Sr}$ ) of carbonates, hydrothermal solutions and river waters. *Geochimica et Cosmochimica Acta* 74 (14), 4097–4109.
- Kuchenbecker, M., 2011. Químioestratigrafia e proveniência sedimentar da porção basal do Grupo Bambuí em Arcos (MG). (Masters Dissertation) Instituto de Geociências da Universidade Federal de Minas Gerais, Belo Horizonte, (91 pp.).
- Kuchenbecker, M., Babinski, M., Pedrosa-Soares, A.C., Costa, R.D., Lopes-Silva, L., Pimenta, F., 2013. Proveniência e análise sedimentar da porção basal do Grupo Bambuí em Arcos (MG). *Geologia USP Série Científica* 13, 49–61.
- Kusnetsov, A.B., Semikhatov, M.A., Gorokhov, I.M., 2012. The Sr isotope composition of world ocean, marginal and inland seas: implication for the Sr isotope stratigraphy. *Sedimentology and Geological Correlation* 20 (6), 501–515.
- Kusnetsov, A.B., Ovchinnikova, G.V., Gorokhov, I.M., Letnikova, E.F., Kaunova, O.K., Konstantinova, G.V., 2013. Age constraints on the Neoproterozoic Baikal Group, from combined Sr isotopes and Pb–Pb dating of carbonates from Baikal type section, southeastern Siberia. *Journal of Asian Earth Sciences* 62, 51–66.
- Li, Z.X., Bogdanova, S.V., Collins, A.S., Davidson, A., De Waele, B., Fitzsimons, I.C.W., Fuck, R.A., Gladkochub, D.P., Jacobs, J., Ernst, R.E., Karlstrom, K.E., Lu, S., Natapov, L.M., Pease, V., Pisarevsky, S.A., Thrane, K., Vernikovsky, V., 2008. Assembly, configuration, and break-up history of Rodinia: a synthesis. *Precambrian Research* 160, 179–210.
- Li, D., Ling, H.F., Shields-Zhou, G.A., Chen, X., Cremonese, L., Och, L., Thirwall, M., Manning, C.J., 2013. Carbon and strontium isotope evolution of seawater across the Ediacaran–Cambrian transition: evidence from Xiaotan section, NE Yunnan, South China. *Precambrian Research* 225, 128–147.
- Martins-Neto, M.A., Hercos, C.M., 2002. Sedimentation and tectonic setting of Early Neoproterozoic glacial deposits in southeastern Brazil. In: Altermann, W., Corcoran, P.L. (Eds.), *Precambrian sedimentary environments: a modern approach to ancient depositional systems*. International Association of Sedimentologists, Special Publications. 33, pp. 383–403.
- Martins-Neto, M.A., Pedrosa-Soares, A.C., Lima, S.A.A., 2001. Tectono-sedimentary evolution of sedimentary basis from Late Paleoproterozoic to Late Neoproterozoic in the São Francisco craton and Araçuaí fold belt, eastern Brazil. *Sedimentary Geology* 142, 343–370.
- Melezlik, V.A., Gorokhov, I.M., Kuznetsov, A.B., Fallack, A.E., 2001. Chemostratigraphy of Neoproterozoic carbonates: implications for “blind dating”. *Terra Nova* 13, 1–11.
- Misi, A., Veizer, J., 1998. Neoproterozoic carbonate sequences of the Una Group, Icre Basin, Brazil: chemostratigraphy, age and correlations. *Precambrian Research* 89, 87–100.
- Misi, A., Kaufman, A.J., Veizer, J., Powis, K., Azmy, K., Boggiani, P.C., Gaucher, C., Teixeira, J.B.G., Sanchez, A.L., Iyer, S.S.S., 2007. Chemostratigraphic correlation of Neoproterozoic successions in South America. *Chemical Geology* 237, 143–167.
- Ohno, T., Komiya, T., Ueno, Y., Hirata, T., Maruyama, S., 2008. Determination of  $^{88}\text{Sr}/^{86}\text{Sr}$  mass-dependent isotopic fractionation and radiogenic isotope variation of  $^{87}\text{Sr}/^{86}\text{Sr}$  in the Neoproterozoic Doushantu Formation. *Gondwana Research* 14, 126–133.
- Ovchinnikova, G.V., Kusnetsov, A.B., Vasil'eva, I.M., Gorokhov, I.M., Letnikova, E.F., Gorokhovskii, B.M., 2012. U-Pb age and Sr isotope signature of cap limestones from the Neoproterozoic Tsagaan Oloom Formation, Dzabkhan River Basin, Western Mongolia. *Geological Correlation* 20 (06), 516–527.
- Palmer, M.R., Edmond, J.M., 1989. The strontium isotope budget of the modern ocean. *Earth and Planetary Science Letters* 92, 11–26.
- Palmer, M.R., Edmond, J.M., 1992. Controls over the strontium isotope composition of river water. *Geochimica et Cosmochimica Acta* 56, 2099–2111.
- Pedrosa-Soares, A.C., Cordani, U.G., Nutman, A., 2000. Constraining the age of Neoproterozoic Glaciation in Eastern Brazil: first U-Pb (SHRIMP) data for detrital zircons. *Revista Brasileira de Geociências* 30, 58–61.
- Pedrosa-Soares, A.C., Alkmim, F.F., Tack, L., Noce, C.M., Babinski, M., Silva, L.C., Martins-Neto, M., 2008. Similarities and differences between the Brazilian and African counterparts of the Neoproterozoic Araçuaí–West Congo Orogen. In: Pankhurst, J.R., Trouw, R.A.J., Brito-Neves, B.B., De Wit, M.J. (Eds.), *West Gondwana: Pre-Cenozoic Correlations Across the South Atlantic Region*. Geological Society of London Special Publications. 294, pp. 153–172.
- Pedrosa-Soares, A.C., Babinski, M., Noce, C., Martins, M., Queiroga, G., Vilela, F., 2011a. The Neoproterozoic Macaúbas Group (Araçuaí orogen, SE Brazil). In: Arnaud, E., Halverson, G.P., Shields-Zhou, G. (Eds.), *The Geological Record of Neoproterozoic Glaciations*. Geological Society, London, Memoirs. 36, pp. 523–534.
- Pedrosa-Soares, A.C., De Campos, C.P., Noce, C., Silva, L.C., Novo, T., Roncato, J., Medeiros, S., Castañeda, C., Queiroga, G., Dantas, E., Dussin, I., Alkmim, F.F., 2011b. Late Neoproterozoic–Cambrian granitic magmatism in the Araçuaí orogen (Brazil), the Eastern Brazilian Pegmatite Province and related mineral resources. *Geological Society of London, Special Publications* 350, 25–51.
- Peixoto, E., Pedrosa-Soares, A.C., Alkmim, F.F., Dussin, I.A., 2015. A suture-related accretionary wedge formed in the Neoproterozoic Araçuaí orogen (SE Brazil) during Western Gondwanaland assembly. *Gondwana Research* 27 (2), 878–896.
- Pimentel, M.M., Fuck, R.A., Botelho, N.F., 1999. Granites and the geodynamic history of the Neoproterozoic Brasília belt, Central Brazil: a review. *Lithos* 46 (3), 463–483.
- Pimentel, M.M., Dardenne, M.A., Fuck, R.A., Viana, M.G., Junges, S.L., Fischel, D.P., Seer, H.J., Dantas, E.L., 2001. Nd isotopes and the provenance of detrital sediments of the

- neoproterozoic Brasília belt, central Brazil. *Journal of South American Earth Sciences* 14 (6), 571–585.
- Pimentel, M.M., Rodrigues, J.B., Della Giustina, M.E.S., Junges, S., Matteini, M., Armstrong, R., 2011. The tectonic evolution of the Neoproterozoic Brasília Belt, central Brazil, based on SHRIMP and LA-ICPMS U-Pb sedimentary provenance data: a review. *Journal of South America Earth Sciences* 31, 345–357.
- Projeto Vida. CPRM – Serviço Geológico do Brasil. 2003. Mapeamento Geológico Região de Sete Lagoas, Pedro Leopoldo, Matozinhos, Lagoa Santa, Vespasiano, Capim Branco, Prudente de Moraes, Confins e Funilândia. Mapa Geológico, scale 1:50,000.
- Queiroga, G.N., Pedrosa-Soares, A.C., Noce, C.M., Alkmim, F.F., Pimentel, M.M., Dantas, E., Martins, M., Castañeda, C., Suita, M.T.F., Prichard, H., 2007. Age of the Ribeirão da Folha ophiolite: the U-Pb zircon (LA-ICPMS) dating of a plagiogranite. *Geonomos* 15 (1), 61–65.
- Rocha-Campos, A.C., Hasui, Y., 1981. Tillites of the Macaúbas Group (Proterozoic) in central Minas Gerais and southern Bahia, Brazil. In: Hambrey, M.J., Harland, W.B. (Eds.), *Earth's Pre-Pleistocene Glacial Record*. Cambridge University Press, pp. 933–939.
- Rodrigues, J.B., 2008. Proveniência de sedimentos dos grupos Canastra, Ibiá, Vazante e Bambuí – um estudo de zircões detriticos e idades Modelo Sm-Nd. (PhD Thesis) Instituto de Geociências, Universidade de Brasília, Brasília, (128 pp.).
- Rodrigues, J.B., Pimentel, M.M., Buhn, B., Matteini, M., Dardenne, M.A., Alvarenga, C.J.S., Armstrong, R.A., 2012. Provenance of the Vazante Group: new U-Pb, Sm-Nd, Lu-Hf isotopic data and implications for the tectonic evolution of the Neoproterozoic Brasília Belt. *Gondwana Research* 21 (2–3), 439–450.
- Santos, R.V., Alvarenga, C.J.S., Dardenne, M.A., Sial, A.N., Ferreira, V.P., 2000. Carbon and oxygen isotope profiles across Meso-Neoproterozoic limestones from central Brazil: Bambuí and Paranoá Groups. *Precambrian Research* 104, 107–122.
- Santos, R.V., Alvarenga, C.J.S., Babinski, M., Ramos, M.L.S., Cukrov, N., Fonseca, M.A., Sial, A.N., Dardenne, M.A., Noce, C.M., 2004. Carbon isotopes of Mesoproterozoic–Neoproterozoic sequences from Southern São Francisco craton and Araçuaí Belt, Brazil: paleogeographic implications. *Journal of South American Earth Sciences* 18, 27–39.
- Sial, A.N., Dardenne, M.A., Misi, A., Pedreira, A.J., Gaucher, C., Ferreira, V.P., Silva Filho, M.A., Uhlein, A., Pedrosa-Soares, A.C., Santos, R.V., Egydio-Silva, M., Babinski, M., Alvarenga, C.J.S., Fairchild, T.R., Pimentel, M.M., 2009. Chapter 3 – The São Francisco Palaeocontinent. In: Gaucher, C., Sial, A.N., Halverson, G.P., Frimmel, H.E., (Org.). *Developments in Precambrian Geology*. 1 ed., London: Elsevier 16, 31–69.
- Silva, L.C., Pedrosa-Soares, A.C., Teixeira, L.R., Armstrong, R., 2008. Tonian rift-related A-type continental plutonism in the Araçuaí Orogen, eastern Brazil: new evidence for the breakup stage of the São Francisco–Congo Paleocontinent. *Gondwana Research* 13, 527–537.
- Silva-Tamayo, J.C., Nägler, T.F., Villa, I.M., Kyser, K., Vieira, L.C., Sial, A.N., Narbonne, G.M., James, N.P., 2010. Global Ca isotope variations in c. 0.7 Ga old post-glacial carbonate successions. *Terra Nova* 22, 188–194.
- Tack, L., Wingate, M.T.D., Liégeois, J.P., Fernandez-Alonso, M., Deblond, A., 2001. Early Neoproterozoic magmatism (1000–910 Ma) of the Zadianian and Mayumbian Groups (Bas-Congo): onset of Rodinian rifting at the western edge of the Congo craton. *Precambrian Research* 110, 277–306.
- Teixeira, W., Kamo, S.L., Arcanjo, J.B.A., 1997. U-Pb zircon and baddeleyite age and tectonic interpretation of the Itabuna alkaline suite, São Francisco Craton, Brazil. *Journal of South America Earth Sciences* 10 (1), 91–98.
- Teixeira, W., Sabaté, P., Barbosa, J., Noce, C.M., Carneiro, M.A., 2000. Archean and Paleoproterozoic tectonic evolution of the São Francisco craton, Brazil. In: Cordani, U.G., Milani, E.J., Thomaz-Filho, A., Campos, D.A. (Eds.), *Tectonic Evolution of South America*. 31st International Geology Congress, Rio de Janeiro, pp. 101–137.
- Tera, F., Wasserburg, G.J., 1972. U-Th-Pb systematics in three Apollo 14 basalts and the problem of initial Pb in lunar rocks. *Earth Planetary Science Letters* 14, 281–304.
- Trindade, R.I.F., D'Agrella-Filho, M.S., Epof, I., Brito-Neves, B.B., 2006. Paleomagnetism of Early Cambrian Itabaiana mafic dikes (NE Brazil) and the final assembly of Gondwana. *Earth and Planetary Science Letters* 244, 361–377.
- Turnipambá, M., Heilbron, M., Valeriano, C., Júnior, R.P., Diós, F.B., Machado, N., Silva, L.G.E., Almeida, J.C.H., 2012. Juvenile contribution of the Neoproterozoic Rio Negro magmatic arc (Ribeira Belt, Brazil): Implications for Western Gondwana amalgamation. *Gondwana Research* 21 (2–3), 422–438.
- Uhlein, A., Trompette, R., Alvarenga, C., 1999. Neoproterozoic glacial and gravitational sedimentation on a continental rifted margin: the Jequitai–Macaúbas sequence (Minas Gerais, Brazil). *Journal of South American Earth Sciences* 12, 435–451.
- Valeriano, C.M., Machado, N., Simonetti, A., Valladares, C.S., Seer, H.J., Simões, L.S.A., 2004. U-Pb geochronology of Southern Brasília belt (SE-Brazil): sedimentary provenance, Neoproterozoic orogeny and assembly of West Gondwana. *Precambrian Research* 130, 27–55.
- Valeriano, C.M., Pimentel, M.M., Heilbrin, M., Almeida, J.C.H., Trouw, R.A.J., 2008. Tectonic evolution of the Brasília Belt, Central Brazil, and early assembly of Gondwana. In: Pankhurst, R.J., Trouw, R.A.J., Brito-Neves, B.B., De Wit, M.J. (Eds.), *West Gondwana: Pre-Cenozoic Correlations Across the South Atlantic Region*. Geological Society, London, Special Publications. 294, pp. 197–210.
- Valladares, C.S., Machado, N., Heilbron, M., Gauthier, G., 2004. Ages of detrital zircon from siliciclastic successions south of the São Francisco Craton, Brazil: implications for the evolution of proterozoic basins. *Gondwana Research* 7 (4), 913–921.
- Veizer, J., Compston, W., Clauer, N., Schidlowski, M., 1983.  $^{87}\text{Sr}/^{86}\text{Sr}$  in Late Proterozoic carbonates: evidence for a mantle event at 900 Ma ago. *Geochimica et Cosmochimica Acta* 47, 295–302.
- Veizer, J., Hoefs, J., Ridder, R.H., Jensen, L.S., Lowe, D.R., 1989. Geochemistry of Precambrian carbonates: I. Archean hydrothermal systems. *Geochimica et Cosmochimica Acta* 53, 845–857.
- Vieira, L.C., Trindade, R.I.F., Nogueira, A.C.R., Ader, M., 2007. Identification of a Sturtian cap carbonate in the Neoproterozoic Sete Lagoas carbonate platform, Bambuí Group, Brazil. *Comptes Rendus Geosciences* 339, 240–258.
- Walter, M.R., Veevers, J.J., Calver, C.R., Gerjan, P., Hill, A.C., 2000. Dating the 840–544 Ma Neoproterozoic interval by isotopes of strontium, carbon, and sulfur in seawater, and some interpretative models. *Precambrian Research* 100, 371–433.
- Warren, L.V., Quaglio, F., Riccomini, C., Simões, M.G., Poiré, D.G., Strikis, N.M., Anelli, L.E., Strikis, P.C., 2014. The puzzle assembled: Ediacaran guide fossil *Cloudina* reveals an old proto-Gondwana seaway. *Geology* <http://dx.doi.org/10.1130/G35304.1>.
- Zhao, Y., Zheng, Y., Chen, F., 2009. Trace element and strontium isotope on sedimentary environment of Ediacaran carbonates in southern Anhui, South China. *Chemical Geology* 265, 345–362.